Aus dem Institut für Physiologie der Universität Tübingen

Abteilung Neurophysiologie

Age-dependent changes in the astrocytic GABA content in a mouse model of Alzheimer's disease

Inaugural-Dissertation
zur Erlangung des Doktorgrades
der Zahnheilkunde

der Medizinischen Fakultät
der Eberhard Karls Universität
zu Tübingen

vorgelegt von

Klement, Daniel Bernhard

2020

Dekan: Professor Dr. B. Pichler

1. Berichterstatter: Professorin Dr. O. Garaschuk
2. Berichterstatter: Privatdozent Dr. M. Krumbholz

Tag der Disputation: 24.7.2020

Table of contents

1. Introduction 6

1.1 Alzheimer's Disease 6

1.2 Astrocytes 8

1.3 Astrocytes can become reactive in AD 9

1.4 Astrocytic influence on neuronal network in aging and AD 11

1.5 Network dysfunction in AD 12

1.6 Astrocytic markers 14

1.7 Mouse models of AD 15

1.8 Summary and Project Aims 16

2. Material & Methods 17

3. Results 21

3.1 Astrocytes in the hippocampus of amyloid-depositing mice show GABA reactivity 21

3.2 Cortical astrocytes show bell-shaped GABA reactivity during amyloidosis 25

3.3 Cortical astrocytes show GABA reactivity exclusively in the vicinity of amyloid plaques 28

3.4 Astrocytic GABA content in the course of healthy aging 31

3.5 Age-dependent differences between WT and AD mice in cortex and hippocampus 38

3.6 GABA reactivity can also be found without the presence of amyloid plaques 43

4. Discussion 47

5. Abstract 53

6. Dt. Zusammenfassung 55

7. Literature 57

8. Declaration of ownership 61

9. Publications 62

10. Acknowledgements 63

Abbreviations

3APS 3-amino-1-propeosulfonic acid
AD Alzheimer's disease
Aldh1L1 aldehyde dehydrogenase 1 family member L1
APO E apolipoprotein E
APP amyloid precursor protein
Aβ amyloid beta
AβPP amyloid precursor protein
Best 1 bestrophin 1
CI's cholesterinase inhibitor's
CNS central nervous system
DG dentate gyrus
EC entorhinal cortex
ECE-2 endothelin-converting enzyme-2
EEG electroencephalogram
FA formaldehyde
FAD familiar Alzheimer's disease
GABA-T gamma aminobutyric acid transaminase
GAD 67 glutamic acid decarboxylase
GAT3/4 GABA transporter protein
GFAP glial fibrilliary acidic protein
GLT1 glutamate transporter 1
GS glutamine synthetase
hAPP human amyloid precursor protein
LOAD "late-onset"- Alzheimer's disease
Maob monoamine oxidase b
mIPSCs miniature inhibitory postsynaptic currents
NDS normal donkey serum
NFTs neurofibrilliary tangles
NMDA N-methyl-D-aspartate
OB olfactory bulb
PBS phosphate buffered saline

PGE_2 prostaglandin-2

PICALM Astrocytic Regulation of Glutamate

PSEN1 presenelin 1

ROI region of interest

S100β S100 calcium-binding protein B

TNFα tumor necrosis factor-α

WT wild type

1. Introduction

1.1 Alzheimer's Disease

With more than 35 million patients worldwide, Alzheimer's disease (AD) is the most common cause of dementia today [1]. At a meeting in Tübingen, Germany, the German psychiatrist Dr. Alois Alzheimer first described neuropathological characteristics of the disease, like neuritic plaques and neurofibrillary tangles (NFTs) in the post mortem brain of a 55-year-old patient. The patient had suffered from severe memory loss and hallucinations [2]. Over the course of the century, it became clear that excessive neuronal loss is accompanied by destruction of functional synapses and perturbations in the excitatory and inhibitory neuronal activity in the AD brain [3, 4].

The NFTs described by Dr. Alzheimer are known to cause neuronal network dysfunction and clinical progression of AD and are built up by the microtubule stabilizing protein tau, which is hyperphosphorylated in AD [5, 6].

Amyloid plaques, which are also known to be a pathological hallmark of AD, are deposits of another protein, amyloid beta (Aβ). Aβ is a by-product of the amyloid precursor protein (APP) processing and arises from the cleavage of the transmembrane protein by β- and γ- secretases [6].

First, β-secretase cleaves the protein at its extracellular domain (β-secretase cleavage), generating β-C-terminal fragments. These fragments are subsequently cleaved by γ-secretase in the transmembrane part of AβPP, resulting in the release of Aβ protein [7]. γ-secretase is able to cut AβPP at multiple sites, producing Aβ proteins of different lengths; i.e. Aβ38, Aβ40 and Aβ42. Aβ42 is the most toxic version and is known to aggregate and to develop amyloid plaques [5, 7-9]. It has been reported that the most pathogenic version of Aβ are soluble oligomeric forms [8]. Also, one of the characteristics of AD, the loss of synapses in the hippocampus and cortex, is considered to be caused by oligomeric Aβ [8].

More than 90% of all AD cases develop clinical symptoms after the age of 65 years. They are often referred to as "sporadic" or "late-onset" AD (LOAD). Genetic factors, like apolipoprotein E4 (APO E4) and Phosphatidylinositol Binding

Clathrin Assembly Protein (PICALM) are further risk factors for developing LOAD [5, 10].

A small percentage (<10%) of all AD cases is hereditary. This form of the disease is called familiar Alzheimer's disease (FAD) and is mainly attributed to mutations in genes encoding amyloid precursor protein (APP), presenilin 1 (PS1) and presenilin 2 (PS2) [5]. While mutations in APP are responsible for overproduction of APP and Aβ [1], mutations in PSEN1 and PSEN2, which are part of the γ-secretase complex, are the cause for an increased Aβ42 cleavage from APP [11]. Several types of therapies exist for the various expressions of the disease, which, however, do not stop the disease but rather slow its progression.

Cholesterinase inhibitors (CIs) can be used as a first line treatment for mild to moderate forms of the disease and are supposed to prevent memory loss and decline of other cognitive and non-cognitive functions. It's believed that cholinergic systems in the basal forebrain are impaired early during disease progression, leading to loss of acetylcholinergic neurons and decreased production of acetylcholine [12].

Moderate to severe forms of AD can be treated with memantine, a non-competitive, moderate-affinity N-methyl-D-aspartate (NMDA) agonist which prevents excitotoxicity in neurons [12].

There is also a so-called disease-modifying approach for AD treatment, targeting the development, increase or elimination of toxic aggregates or misfolded forms of Aβ and tau. Examples are the synthetic glycosaminoglycan 3-amino-1-propeosulfonic acid (3APS) tramiprosate, which is supposed to hinder the binding of glycosaminoglycanes and Aβ, or β-secretase inhibitors like methylene blue [12]. Behavioral symptoms of the disease can be treated by the use of an antipsychotic and an antidepressant at the same time [12].

All of these treatments are only symptomatic, trying to counterbalance the neuronal disturbance, and to date no cure for AD is known. Therefore, it's necessary to understand the mechanisms underlying the origin and the progression of the disease in its complexity, so that improved treatment options can be developed in the future.

1.2 Astrocytes

Astrocytes are glial cells and part of the central nervous system (CNS). They were named astrocytes by Michael von Lenhossek in 1895 due to their numerous processes, which give them a star-shaped cell structure. This morphology also allows to differentiate them from other glial cells like microglia and oligodendroglia [6].

Later, astrocytes were subdivided into fibrous and protoplasmic forms. Protoplasmic astrocytes are located in the gray matter and interact with neurons at pre- and postsynaptic elements, while fibrous astrocytes are located in the white matter and interact with myelinated axons [6, 13].

With the emergence of the extracellular matrix receptor CD44 as an astrocytic marker, several other astrocytic subpopulations have been found, such as a mixed protoplasmic and fibrous phenotype with long processes [6].

While it was originally thought that astrocytes were non-excitable cells that were mere „brain glue“ and had only supporting function [14], this view has changed over the past decades. Astrocytes are key for almost every vital CNS function, including neurogenesis, synapse development and function, regulation of blood flow, energy metabolism, ion and water homeostasis, proper function of the blood brain barrier and neurotransmission [13].

In addition, astrocytes play an important role in preventing glutamate-induced excitotoxicity, as they can take up glutamate from the synaptic cleft via amino acid transporters like glutamate transporter 1 (GLT1). Subsequently, glutamate is metabolized into glutamine by glutamine synthetase and transferred to the presynaptic neuron [15].

Astrocytes also possess enzymes like glutamic acid decarboxylase (GAD 67) and gamma aminobutyric acid transaminase (GABA-T), which allow them to synthesize and metabolize GABA. The ability to also release the neurotransmitter via bestrophin 1 (Best 1) channels show that they also play an important role in maintaining GABA levels [15, 16].

In summary, astrocytes play an important role in regulating brain homeostasis and activity, and disease-related impairment of their abilities or malfunction can lead to or aggravate brain pathologies.

1.3 Astrocytes can become reactive in AD

As previously mentioned, under physiological conditions astrocytes have a star-like appearance, whereas under pathological conditions, like brain injury, stroke or AD, astrocytes can become reactive.

There are several markers for a reactive astrocytes, including cell hypertrophy, increased intracellular concentration of glial fibrillary acidic protein (GFAP) and S100 calcium-binding protein β (S100β) as well as expression and release of inflammatory mediators [6, 17]. In AD, these changes are caused by Aβ toxicity, which causes activation of the astrocytes assembling in the vicinity of amyloid plaques [18].

In addition, activated microglia, representing the first line of defense under conditions of brain damage, release cytokines like tumor necrosis factor-α (TNFα), interleukin-1 and prostaglandin-2 (PGE_2) that can also lead to astrocyte reactivity [17].

Reactive astrocytes try to shield the surrounding neuropil from amyloid plaques using their processes, and postmortem neuropathological studies have found an excessive number of reactive astrocytes were found in the vicinity of amyloid plaques not depending on plaque size [6]. In addition, it has been proven that endothelin-converting enzyme-2 (ECE-2), an enzyme that is able to degrade Aβ, is upregulated in astrocytes in AD, which implies that astrocytes also play a role in limiting the growth of amyloid plaques [19].

As reported by Jo et al. (2014) and Wu et al. (2014), GABA content of reactive astrocytes in the dentate gyrus (DG) of the hippocampus is higher in amyloid-depositing mice compared to WT mice of the same age [16, 20]. Functionally, this accumulation induces increased tonic inhibition of the DG network via abnormal GABA release by astrocytes, which ultimately results in memory deficits [16, 20].

While both studies described similar results, they described different mechanisms underlying the effects observed.

One difference is the choice of AD mouse models and the different age of experimental animals under study. Wu et al. used 5xFAD mice and found an increase in GABA accumulation and release from astrocytes at 6-8 months, while Jo et al. observed increased astrocytic GABA content and release in 8-13 months old APPswe/PSEN1dE9 mice.

Of note, only Jo et al. report a positive correlation between astrocytic GABA content and the distance to amyloid depositions, with astrocytes further than 80 µm away showing GABA content similar to astrocytes in control mice. Wu et al. describe no such correlation.

The most important difference, however, refers to mechanisms of GABA accumulation in and release from astrocytes.

Jo et al. (2014) argued that the elevated GABA levels are caused by an increased GABA production via monoamine oxidase b (Maob) and that GABA is subsequently released via Best 1 channels [20]. Wu et al. (2014) proved that GABA is released via GABA transporter protein (GAT3/4) and assumed that since expression of GAD67 was increased in reactive astrocytes in AD mice compared to WT mice, GAD67 may be one of the reasons for GABA accumulation in astrocytes [16].

As mentioned above, both groups studied astrocytes in the DG of the hippocampus. So far, it is unknown if increased GABA content can also be found in reactive astrocytes in other brain regions. An object of interest would be the frontal cortex, an area that is also affected by Aβ pathology and is important for learning, memory and other cognitive processes [18, 21, 22].

Moreover, it remains unknown whether astrocytic GABA accumulation solely represents an early biomarker of pathology or, in contrary, the astrocytic GABA content increases with the progression of the disease.

1.4 Astrocytic influence on neuronal network in aging and AD

As mentioned above, astrocytes are able to release neurotransmitters like glutamate and GABA. The release of these neurotransmitters is correlated with an increased intracellular calcium concentration in astrocytes and can trigger small inward or outward currents in surrounding neurons [17, 18, 23]. Therefore, it's likely that neurotransmitters released by astrocytes play an important role in maintaining physiological levels of neuronal network activity.

In a study by Banuelos et al. (2014), it was suggested that age-dependent working memory impairment is linked to disturbances in cortical GABA release by astrocytes [24]. The authors investigated WT rats at 6 months and 22 months of age and found that the expression of the GABA synthetizing enzyme GAD 67 was severely increased. GAD 67 is a catalyst for the conversion of glutamate to GABA in both neurons and astrocytes. Also, a decrease in the $GABA_B$ receptor subunits, which restrict GABA release from interneurons, and a reduced expression of the GABA transporter protein (GAT3/4), which removes GABA from the synaptic cleft and transports it back to the presynaptic terminal, was found [24]. This leads to the assumption that an increase in GABA synthesis and prolongation of GABA at the synaptic cleft may be responsible for working memory deficits in the prefrontal cortex of aged rats. Furthermore, this can be viewed as a hint that astrocytic neurotransmitter release plays a role in regulating neuronal networks since GAD67 is present and upregulated in astrocytes.

Mitew et al. (2013) report that GAD67 was more active in APP/PS1 transgenic AD mice than in age-matched WT mice. However, this was only found in cortical astrocytes in AD mice acquired from purified glial synaptosome extracts.

Since astrocytes express GAD67 and increased GAD67 activity was seen in glial tissue extracts, these data may serve as a further indication for the important role astrocytes play in maintaining neuronal network activity [25].

Furthermore, astrocytes are able to activate neighboring neurons by upregulation of glutamatergic transmission and the release of TNF-α [26, 27].

To sum it all up, astrocytes have widespread influences on maintaining functional neuronal networks. This influence seems to be altered during the aging process.

1.5 Network dysfunction in AD

A growing number of studies report neural network hyperactivity in both humans and mouse models of AD. As reported by Palop et al. (2009), in patients aberrant cortical network activity can be seen in both the sporadic and inherited form of the disease [4].

Non-convulsive epileptic-like seizures, which may be a cause of clinical symptoms of AD like disorientation and amnesia, have been observed during electroencephalogram (EEG) recordings in the hAPPJ20 mouse model of FAD. As a compensation for this activity, inhibitory circuits were remodeled in the hippocampus [28]. Furthermore, an increase in neuropeptide-Y levels as well as enlarged GABAergic miniature inhibitory postsynaptic currents (mIPSCs) were found in the DG [28].

Busche et al. (2008) found a difference in the percentage of hyperactive and hypoactive neurons in a mouse model of AD compared to wild type (WT) mice at the same age. At 6-10 months of age, they found higher fractions of both hyperactive and hypoactive cortical neurons in AD mice compared to age-matched control mice [22]. Also, AD mice performed worse than control mice in memory tests. At that time, this finding contradicted the accepted belief that neuronal network activity is decreased in AD brain.

Additionally, the authors found a connection between hyperactive neurons and amyloid plaques. While hyperactive neurons were only found within a radius of 60 µm of the nearest plaque, hypoactive neurons were found throughout the parenchyma [22]. The activity of hyperactive neurons was decreased by the application of diazepam, a benzodiazepine that increases the open probability of $GABA_A$ receptors [22].

Network dysfunction during amyloidosis has also been found in the hippocampus. Busche et al. (2012) revealed that in the hippocampus of 2-month-old, the percentage of hyperactive neurons is 24% higher in AD mice than in age matched WT mice [29]. The number of hyperactive neurons then decreased by 16.4% in AD from 1-2 months old mice to 6-7 old mice yet continued to be 6.6% higher than in age matched control mice. The percentage of hypoactive neurons was

also higher in AD mice at 6-7 months of age compared to control mice [29]. However, in this case the increase in neuronal network activity was not caused by amyloid plaques, since at this young age no plaques have developed in the hippocampus yet. The authors found that the presence of soluble Aβ was the reason for hyperactivity of neurons and proved that administration of a γ-secretase inhibitor subsequently leads to a decrease in soluble Aβ levels and normalized neuronal activity. Consistently, administration of soluble Aβ lead to neuronal hyperactivity in WT mice [29].

Another part of the mouse brain where similar results have been found is the visual cortex. A study by Grienberger et al. (2012) observed an increase in hyperactive and hypoactive neurons in the visual cortex of AD mice, as well as an impaired performance in a visual discrimination test.

Hyperactive neurons were impaired in their tuning properties, as suggested by reduced orientation and direction selectivity to visual stimuli [30].

Neurons in the visual cortex returned to normal tuning after application of the $GABA_A$ receptor agonist Gabazine [30].

Recent studies reported neuronal hyperactivity also in mutant mice without amyloid plaques or neuroinflammation, like mice carrying solely the $PS1_{G384A}$ mutation (hereafter referred to as “PS45” mice) [31, 32]. Furthermore, Lerdkrai et al. (2018) not only showed that neuronal hyperactivity can occur in the absence of amyloid plaques, but also during the aging process in WT mice [32].

Asavapanumas et al. (2018) also observed neuronal hyperactivity in the visual cortex of AD and PS45 mice [33]. They labeled all recorded neurons as either silent, normal or hyperactive and found impairments in orientation and direction selective tuning not only in hyperactive neurons, as reported by Grienberger et al. (2012), but also in normal neurons in 10-12 months old AD and PS45 mice [33].

Taken together, besides the well-known morphological reactivity of astrocytes in the course of AD, there is also a profound disturbance of neuronal networks. Both of these pathological events occur in the close vicinity of amyloid plaques. However, if they are initiated by the same factors and how these alterations develop in the course of amyloidosis remains to be determined.

1.6 Astrocytic markers

There are several markers for astrocytes, with the most established ones being GFAP, S100β and Glutamine Synthetase (GS). To date, no astrocytic marker exists that is able to reflect the full heterogeneity of astrocytes. Recently, a new alternative, Aldehyde dehydrogenase 1 family member L1 (Aldh1L1), was developed that may in the future allow to distinguish between the various astrocytic forms [34].

1.6.1 GFAP

Since its discovery in 1969, GFAP has become one of the most reliable markers for astrocytes in the brain [35], However, it works well in many but not all regions of the brain and is mostly labelling astrocytic processes [34]. GFAP is found in aged as well as in juvenile astrocytes and is known to be elevated in damaged or degenerated brains [36].

1.6.2 S100β

The Ca^{2+} binding protein S100 has multiple paracrine trophic effects in the CNS and can also be used to specifically label astrocytes using immunohistochemistry [37]. We chose an anti-S100β antibody for our study because it produced an adequate staining of astrocytic cell body and processes. However, S100β also labels other glial cells, for example a subpopulation of oligodendrocytes [38].

1.6.3 GS

GS is responsible for nitrogen metabolism and most importantly metabolism of the amino acid neurotransmitters glutamic acid and γ-aminobutyric acid. It has been shown that GS is exclusively expressed in astrocytes [39].

1.6.4 ALDH1L1

Aldh1L1 is an enzyme that metabolizes 10-formyltetrahydrofolate to tetrahydrofolate and plays an important role in de novo nucleotide biosynthesis, cell division and growth. Adh1L1 is present in almost all astrocytes, but no other CNS cells, which qualifies it as a superior marker to distinguish astrocytes from other glial cell types [34].

1.7 Mouse models of AD

There are numerous transgenic mouse models that express pathological features of AD, like cognitive and behavioral deficits, plaque formation and NFTs. However, a mouse model that shows all characteristics associated with AD does not exist yet as symptoms differ in degree and combinations [1]. For our study, we used the following two mouse models.

1.7.1 APP23xPS45 double transgenic mice

APP23xPS45 is a double transgenic mouse line generated by crossing APP23 mice, carrying the Human App Swedish (670/671) mutation [40] with PS45 mice, carrying the Human G384A-mutated PS1 [41].
In these mice, deposition of senile plaques starts at ~ 6 weeks of age in the neocortex and at 2-3 months of age in the hippocampus (DG) and is followed by gliosis (hypertrophic astrocytes) at 6 months of age [42]. Mice show full blown plaque pathology in the cortex at an age of 8 months [43].
The combination of these mutations leads to a high production of Aβ42, an impairment in cognitive functions and a reduced performance in the water maze test of mice at 6-8 months of age [22].

1.7.2 PS45 mouse model

PS45 mice overexpress human G384A-mutated PS1. Although this mutation also increases the production of Aβ42 [44], PS45 mice do not develop plaque pathology, neuroinflammation and do not show behavioral or cognitive alterations [41]. However, at 10-14 months of age PS45 mice exhibit a hyperactivity of neurons, comparable to disturbances in neuronal network in AD mice at the same age [32].

1.8 Summary and Project Aims

In summary, there is evidence for a positive correlation between amyloidosis and an altered GABA content in astrocytes surrounding amyloid plaques in the hippocampus. Different studies have shown that pathological GABA release from astrocytes under these circumstances can affect neuronal network activity leading to tonic inhibition in the hippocampus. However, it is unclear whether astrocytes accumulate GABA also in other brain regions during amyloidosis and how the enhanced GABA content changes during disease progression. Furthermore, it is not known if astrocytic GABA content is also affected during the mild inflammatory reaction, which is found in the aged brain.

In the current project we aimed at filling these gaps by asking following specific questions:

1. Does astrocytic GABA accumulation take place exclusively in the hippocampus or can this phenomenon be found in other areas of the brain in AD mice?
2. Is GABA accumulation in astrocytes linked to the aging process in WT mice?
3. Does GABA reactivity of astrocytes depend on the presence of amyloid plaques?

2. Material & Methods

Mice

All experimental procedures were performed in accordance with regulations set by the government of Baden-Württemberg, Germany (PY 7/08, PY 1/16, PY 3/13, PY 9/11).

1-2 months (n=5), 4-6 months (n=5) and 9-10 months old (n=5) transgenic APP23xPS45 mice, age-matched WT C57BL/6 mice (2 months, n=5; 4-6 months, n=5; 9-11 months, n=6) and PS 45 mice (4-6 months, n =5) were used for experiments. Also, WT C57BL/6 mice (n=5) at 18-20 months of age were used.

Both APPx23PS45 mice and PS45 mice were raised on a C57BL/6 background. APP23xPS45 is a double transgenic mouse line which is generated by crossing APP23 mice, carrying the human APP Swedish (670/671) mutation [40] with PS 45 mice, carrying the Human G384A-mutated PS1 [41]. Expression of these mutated genes, which also lead to dementia in humans, cause the enhanced production of $A\beta_{42,}$ a toxic form of amyloid that is highly prone to aggregation.

Deposition of senile plaques starts at 6 weeks of age in the neocortex and at 2-3 months of age in the hippocampus (DG). Mice show full blown plaque pathology in the cortex at an age of 8 months [43]. At an age of 6-8 months, mice exhibit impairment in cognitive functions as shown by reduced performance in the water maze test [22]. PS 45 mice, carrying the Human G384A-mutated PS1, do not develop plaque pathology and show no behavioral or cognitive alterations [41].

All mice were housed in the animal facility at the Pharmacology and Toxicology Institute, University of Tübingen. Mice had free access to food and water and were kept under a 12-hour light/ dark cycle.

Tissue preparation

Transcardial perfusion was performed to preserve the integrity of the brain tissue. Mice were anesthetized by intraperitoneal injections of Ketamine (50 mg/ml) and Xylazine (20 mg/ml) at a ratio of 1:1, depending on the animal's weight (10 mg/kg bodyweight).

Mice were transcardially perfused with cold phosphate buffered saline (PBS), followed by 4% formaldehyde (FA). Afterwards, the brain was removed and placed in 4% FA at 4°C overnight. After deposition in 25% sucrose for 24 hours, the brain was embedded in Tissue-Tek (Tissue Tek®) and frozen on dry ice. Tissue was kept at -80 C° until further use.

Immunohistochemistry

Sagittal brain slices of 50 µm thickness were cut using a cryotome (Leica CM1950). Slices were washed in PBS, blocked in 10% normal donkey serum (NDS) for 2 hours at room temperature, and transferred to the primary antibody solution (primary antibody in 2% NDS/ 1% Triton-x-100/ PBS) for 60 hours at room temperature. The primary antibodies used in our protocol were mouse anti-S100β (Abcam) at a dilution of 1:200 and rabbit anti-GABA (Immunostar) at a dilution of 1:2000.

Next, slices were washed in PBS and transferred into the secondary antibody solution (secondary antibody in 2% NDS/ 1% Triton-x-100/ PBS) for 1,5 hours. Secondary antibodies used were donkey anti-mouse 488 (Mobitec) at a dilution of 1:200 and donkey anti-rabbit Alexa 594 (Invitrogen) at a dilution of 1:1000.

Slices were washed in PBS and mounted on glass slides with VectaShield mounting media (Vector laboratories). Glass coverslips were fixed to superfrost glass slides with nail varnish around the edges. Fibrillar amyloid deposits were visualized by counterstaining slices with $1x10^{-6}$ Thioflavin-S (Sigma-Aldrich) in PBS for 5 minutes.

Imaging and Analysis

Two-photon images of immunofluorescent antibody staining were recorded with an x40 water immersion objective (Zeiss), 0.8 N.A., in the cortex, hippocampus and olfactory bulb (OB) using a custom-built two-photon laser scanning microscope, with a mode-locked laser (MaiTai, Spectra Physics) working at 690-1040 nm. The laser was connected to an Olympus FV300 laser scanning system and an Olympus BX51WI microscope.

All fluorophores were excited at 800 nm and emitted light was collected with two separate photomultiplier tubes. Emitted light from S100β-Alexa488 and GABA-Alexa594 was collected using a 585 nm secondary dichroic mirror, splitting emitted light into two channels. Additionally, a 536/40 nm bandpass filter and a 568 nm longpass filter were used to exclude the emission light with the wrong wavelength. Fluorescence from S100β-Alexa488 was collected by PMT1, while fluorescence from GABA-Alexa594 was collected by PMT2.

Emitted light from Thioflavin-S was collected by using a different secondary dichroic mirror (515 nm). Emitted light was collected in the 420-520 nm wavelength range by using an additional barrier filter. Additionally, a 470/100 nm bandpass filter was used to exclude the emission light with the wrong wavelength. 512x512 pixel, 16-bit z-stack TIFF images were acquired at x 2 magnification, 1 µm z-axis intervals and averaged over 3 frames.

To measure GABA intensity in astrocytes, maximum GABA intensity projection images were created with 4-12 slice thick z-stack images for every analyzed cell. The top and bottom slice where the cell of interest appears first determined the boundaries of the z-stack. Next, a region of interest (ROI) was drawn around the astrocyte in the S100β channel. Subsequently, three background ROIs were drawn in the GABA channel and fluorescence intensity of all four ROIs was measured in the GABA channel.

Normalized GABA intensity was calculated as follows:

Normalized GABA intensity = cell GABA intensity / average background intensity

Image analysis and analysis were made in Fiji (*https://imagej.net/Fiji*).

Defining different cell types

In the 4-6 months age group of AD mice, astrocytes were divided into two different groups, depending on their distance from the nearest amyloid plaque. As various pathological alterations in different cell types have been described to occur within a radius of 50-60 µm from amyloid plaques [22, 45], we chose to define the area located ≤ 60µm from plaques as plaque vicinity.

Astrocytes that were located ≤ 60 µm from the nearest plaque were defined as “near the plaque” cells and astrocytes that are located > 60 µm from the nearest

plaque were defined as “far from plaque” cells. The 60 µm radius was set from the edge of the plaque to the centre of the cell somata. A plaque was defined as a Thioflavin-S positive amyloid deposit if its diameter exceeded 5 µm.

Statistics

Statistical analyses were performed using the VassarStats Statistical Computation Website (http://vassarstats.net/), Excel (Microsoft, Redmond, WA, USA), and MATLAB (The MathWorks, Natick, MA, USA). Data are shown as median ± interquartile range, if not indicated otherwise. Lines of box plots represent 25th and 75th, whiskers 10th and 90th percentiles.

Shapiro-Wilk test was used to test data sets for normality. As all relevant data sets were distributed normally, Student's t-test was used for comparison of two data sets. For comparison of three data sets, one-way ANOVA followed by a post-hoc Bonferroni correction for multiple comparisons was used for normally distributed data, and Kruskal-Wallis test followed by a post-hoc Dunn’s correction for multiple comparisons was used for data that was not normally distributed. Differences between the groups were regarded as significant if p-values were below 0.05. Spearman's rank correlation coefficient (rS) was used to analyze the correlation between soma size and GABA intensity. If p-values were below 0.05, correlation was regarded as significant.

Distribution of astrocytic soma size and GABA intensity in the analyzed population of cells was compared between different groups using the Kolmogorov-Smirnov test. Differences between the groups were regarded as significant if p-values were below 0.01.

3. Results

In this study, size and GABA content of astrocytes in cortical layers 2/3, olfactory bulb and DG of amyloid-depositing and WT mice were examined in fixed brain slices using two-photon microscopy. Since we aimed to observe plaque-dependent changes in astrocytes we chose the following age groups: 1-2 months, at this age no plaque depositions have developed yet; 4-6 months, starting phase of plaque deposition; and 9-11 months, where plaques are vastly abundant throughout the cortex and DG. We also included 18-20 months old WT mice, allowing us to make observations about astrocytic changes during the healthy aging process.

We analyzed soma size and GABA content, as they are well-known parameters characterizing a reactive astrocyte and are known to be affected by amyloidosis.

3.1 Astrocytes in the hippocampus of amyloid-depositing mice show GABA reactivity

First, we examined hippocampal astrocytes of amyloid-depositing mice, as it has been shown that astrocytic GABA reactivity can be found in this brain region in other mouse models of AD.

In images of 4-6 months and 9-11 months old mice (Fig. 1, middle and lower row), astrocytes could clearly be identified in the GABA channel (red; second and third row) and a colocalization of S110β (green) and GABA could be seen in the merged images on the right. Furthermore, Thioflavin-S positive plaque formations were evident (blue; third row) as mice age, while no amyloid plaques and colocalization could be found in 1-2 months old mice (upper row).

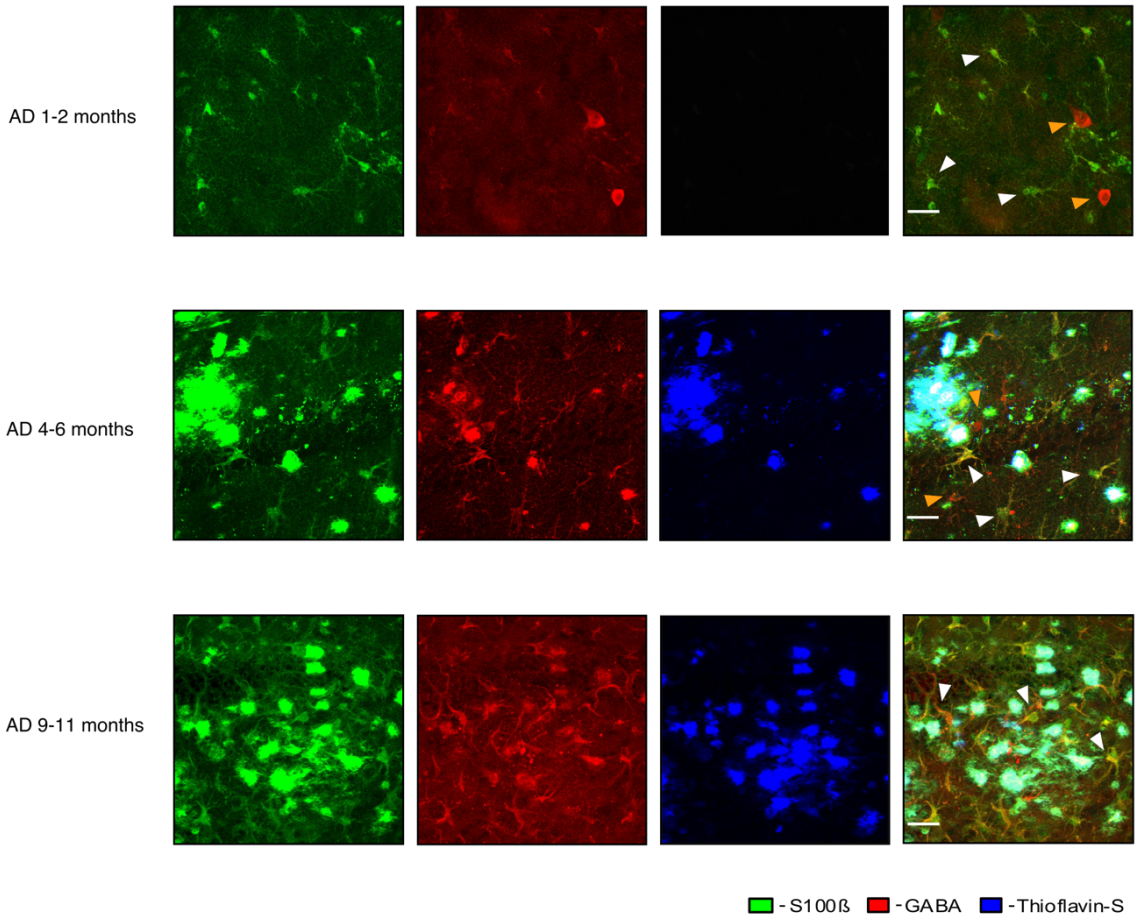

Figure 1: Hippocampal astrocytes of amyloid-depositing mice show significant GABA reactivity. Maximum-intensity projection obtained from the hippocampus (DG) in a fixed brain slice of an amyloid-depositing mouse at 2 months (upper row, 15 slices, step size 1 µm), 6 months (middle row, 15 slices, step size 1 µm) and 11 months (bottom row, 14 slices, step size 1 µm) of age, respectively. Brain slices were labeled with antibodies against S100β (green; left panel), GABA (red; middle panel) and with Thioflavin-S (blue; right panel). In the merged images on the right, S100β-positive astrocytes are indicated by white arrows and GABA-positive interneurons are indicated by orange triangles. Scale bar 20 µm.

We found a trend towards increase in median (per mouse) soma size in the course of amyloid deposition, however, this trend did not reach statistical significance (Fig. 2A left panel; p= 0.308, one-way ANOVA). Comparing median normalized GABA intensity between different age groups, we not only found an astrocytic accumulation of GABA at 4-6 months, as previously reported, but also an up-and-down trend in GABA values with a significant increase from 1-2 months to 4-6 months (Fig. 2A right panel; $p < 0.01$*; one-way ANOVA followed by a post-hoc Bonferroni correction for multiple comparisons) and a significant decrease from 4-6 months to 9-11 months (Fig. 2A right panel; $p<0.01$*; post-hoc

Bonferroni correction for multiple comparisons). A difference between astrocytic GABA levels in 1-2 months and 9-11 months old mice was not significant ($p=0.361$; post-hoc Bonferroni correction for multiple comparisons).

Cumulative distribution of soma size showed a similar development with a shift to the right from 1-2 months to 4-6 months (Fig. 2A left panel; $p<0.01$*, Kolmogorov-Smirnov test), while there was no significant difference between 4-6 months and 9-11 months ($p=0.02$).

A prominent shift was also visible from 1-2 months to 9-11 months ($p<0.01$, Kolmogorov-Smirnov test).

For normalized GABA intensity, an up-and-down trend was visible with a prominent shift to the right solely in the 4-6 months age group, then dropping to lower values in 9-11 months old mice (Fig. 2B, right panel; $p<0.01$* for all comparisons, Kolmogorov-Smirnov test).

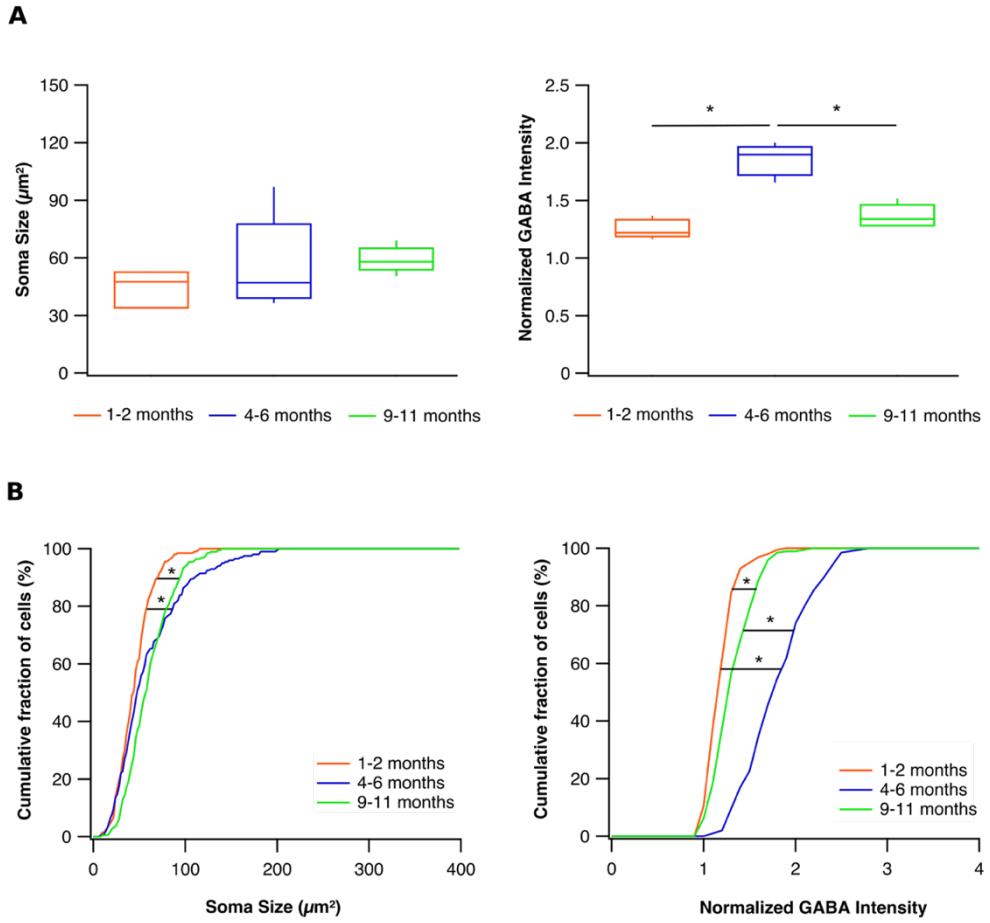

Figure 2: In amyloid-depositing mice, hippocampal astrocytes show significant changes in soma size and GABA content throughout the aging process. This figure was reproduced from Brawek et al. (2018) [46].
A: Box-and-whisker plots showing median soma size (left) and normalized GABA intensity (right) of hippocampal astrocytes in amyloid-depositing mice at 1-2 months (red; n=5 mice), 4-6 months (blue; n=5 mice) and 9-11 months (green; n=5 mice) of age. Both soma size and normalized GABA intensity increased from 1-2 months old mice to 4-6 months old mice, then decreased in the 9-11 months age group ($p=0.308$ for "soma size"; $p<0.01$* for "normalized GABA intensity", 1-2 vs 4-6 and 4-6 vs 9-11 $p<0.05$*, 1-2 vs 9-11 $p=0.361$; one-way ANOVA).
B: Distribution of soma size (left) and normalized GABA intensity (right) of hippocampal astrocytes in amyloid-depositing mice at 1-2 months (red; 200 cells), 4-6 months (blue; 199 cells) and 9-11 months (green; 195 cells) of age, displayed by cumulative probability histograms. Compared to 1-2 months old mice, 4-6 months and 9-11 months old mice reached higher values in soma size. GABA intensity was strongly shifted from 1-2 months to 4-6 months old mice, then back to lower levels in the 9-11 months age group (1-2 vs 4-6 and 1-2 vs 9-11 $p<0.01$*, 4-6 vs 9-11 $p=0.02$ for "soma size"; $p<0.01$* for "Normalized GABA intensity"; Kolmogorov-Smirnov-Test).

These results show a bell-shaped dependence of GABA content in hippocampal astrocytes on mouse age and suggest that GABA accumulation and cell hypertrophy are regulated by separate mechanisms.

3.2 Cortical astrocytes show bell-shaped GABA reactivity during amyloidosis

To find out whether this observation is only true for the DG or if it also true for other parts of the mouse brain, we examined astrocytes in the frontal cortex of AD mice, since this region undergoes strong amyloidosis both in mice and humans.

Again, there was plaque formation and colocalization of S100β and GABA reactivity in the plaque vicinity in images of 4-6 months and 9-11 months old mice (Fig. 3A, third and fourth row), while none was visible in 1-2 months old animals (first row).

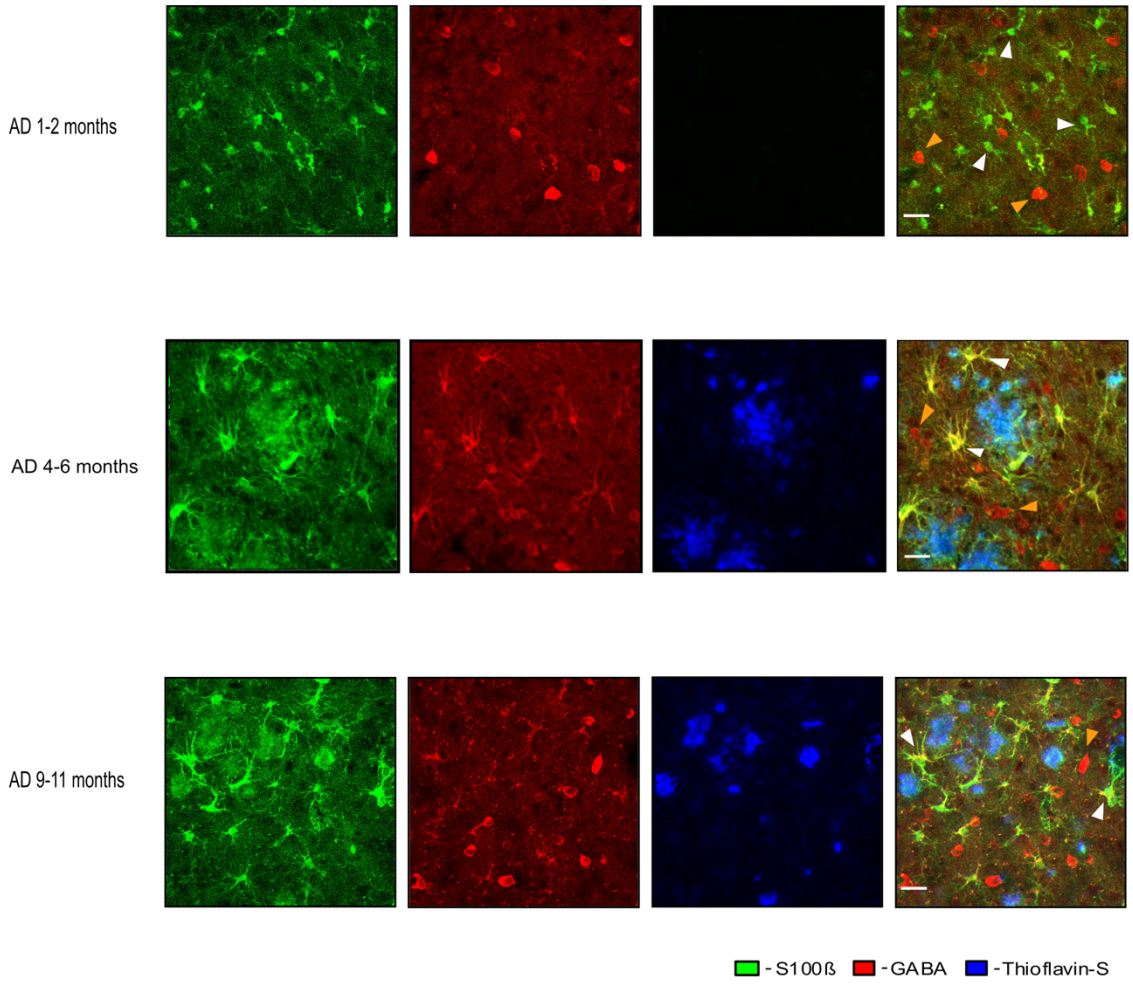

Figure 3: Cortical astrocytes of amyloid-depositing mice show significant GABA reactivity. Maximum-intensity projection images obtained from the frontal cortex in a fixed brain slice of an amyloid-depositing mouse at 2 months of age (upper row, 14 slices, step size 1 µm), 6 months (middle row, 12 slices, step size 1 µm) and 11 months of age (bottom row, 18 slices, step size 1 µm). Brain slices were labeled with antibodies against S100β (green; left panel), GABA (red; middle panel) and with Thioflavin-S (blue; right panel). In the merged images on the right, S100β-positive astrocytes are indicated by white triangles and GABA-positive interneurons are indicated by orange triangles. Scale bar 20 µm.

We found that median soma size increased continuously with age, with a significant difference between 1-2 months age group and both 4-6 months and 9-11 months age groups, and no difference between 4-6 months and 9-11 months age groups (Fig. 4A, left panel; 1-2 months vs. 4-6 months and 1-2 months vs. 9-11 months $p<0.01$*, 4-6 vs. 9-11 $p=0.661$; one-way ANOVA). Similar to the data obtained for DG, median GABA intensity also increased significantly from 1-2 months to 4-6 months (Fig. 4A, right panel; 1-2 vs. 4-6 $p<0.01$*; one-way ANOVA) yet decreased significantly from 4-6 months to 9-11 months of age (Fig. 4A, right

panel; 4-6 vs. 9-11 p<0.01*; one-way ANOVA). A difference between GABA levels in 1-2 months and 9-11 months was not detectable (Fig. 4A, right panel; 1-2 vs. 9-11 p=1; one-way ANOVA). Comparing the different age groups on the population level endorsed the notion that soma size increases in the course of aging (Fig. 4B, left panel; p<0.01*; Kolmogorov-Smirnov test). On the other hand, normalized GABA intensity values showed an up-and-down trend with the highest values observed in 4-6 months old mice (Fig. 4B, right panel; p<0.01* for all comparisons; Kolmogorov-Smirnov test).

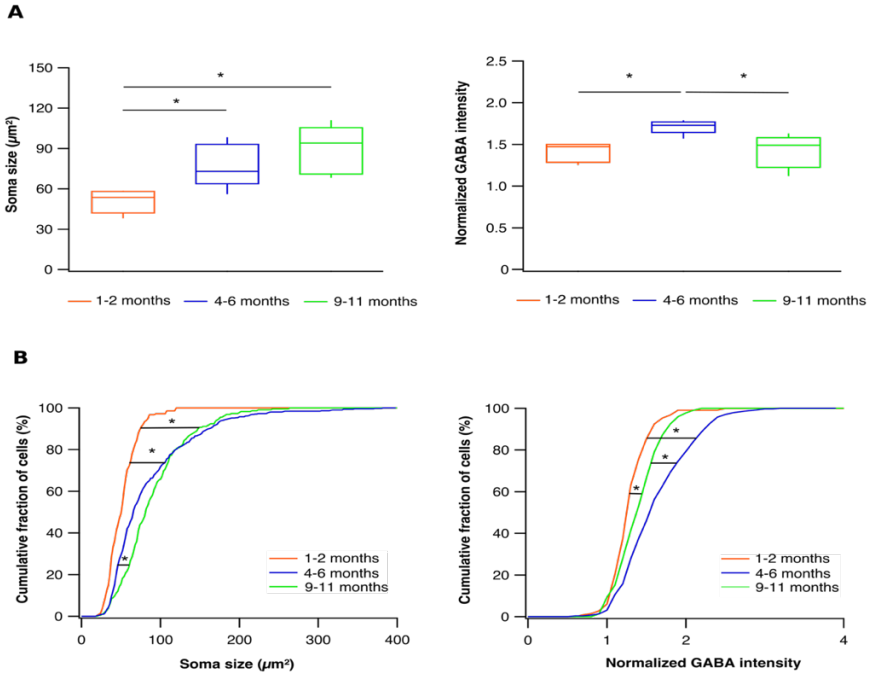

Figure 4: In amyloid depositing mice, cortical astrocytes show significant changes in soma size and GABA content throughout the aging process. This figure was reproduced from Brawek et al. (2018) [46].
A: Box-and-whisker plots showing median soma size (left) and normalized GABA intensity (right) of cortical astrocytes in amyloid-depositing mice at 1-2 months (red; n=5 mice), 4-6 months (blue; n=5 mice) and 9-11 months (green; n=5 mice) of age. Soma size continuously increases with age, while there was a clear up-and-down trend in normalized GABA intensity (1-2 vs 4-6 and 1-2 vs 9-11 p<0.01*, 4-6 vs 9-11 p=0.661 for "soma size"; 1-2 vs 4-6 and 4-6 vs 9-11 p<0.01*, 1-2 vs 9-11 p=1 for "normalized GABA intensity"; one-way ANOVA).
B: Distributions of soma size (left) and normalized GABA intensity (right) of cortical astrocytes in amyloid-depositing mice at 1-2 months (red; 213 cells), 4-6 months (blue; 513 cells) and 9-11 months (green; 225 cells) of age, displayed as cumulative probability histograms. Compared to 1-2 months old mice, soma size increased in both 4-6 months and 9-11 months old mice (p<0.01*; Kolmogorov-Smirnov-Test). GABA intensity increased strongly from 1-2 months to 4-6 months old mice (p<0.01*; Kolmogorov-Smirnov-Test), then reached lower levels in the 9-11 months age group (p<0.01*; Kolmogorov-Smirnov-Test).

These results show a bell-shaped development of GABA content in astrocytes during the course of amyloidosis in the frontal cortex, comparable to that seen in the DG, again suggesting that during aging GABA accumulation and cell hypertrophy are regulated by separate mechanisms.

3.3 Cortical astrocytes show GABA reactivity exclusively in the vicinity of amyloid plaques

Next, we decided to elaborate on possible reasons for hypertrophy and GABA reactivity in cortical astrocytes of amyloid-depositing mice at 4-6 months of age. Therefore, we classified astrocytes dwelling at a distance less than 60 µm from the nearest amyloid deposition as located in “plaque vicinity“ and those located more than 60 µm away as “far from plaque“ and measured GABA intensity and soma size (Fig. 5).

Because at 4-6 months the plaque deposition in the frontal cortex of amyloid-depositing mice is present but not ubiquitous, this age group was chosen to distinguish between astrocytes close and far from plaques. In contrast, at an age of 9-11 months plaques were vastly abundant throughout the cortex and virtually all astrocytes were located less than 60 µm away from the closest amyloid deposition.

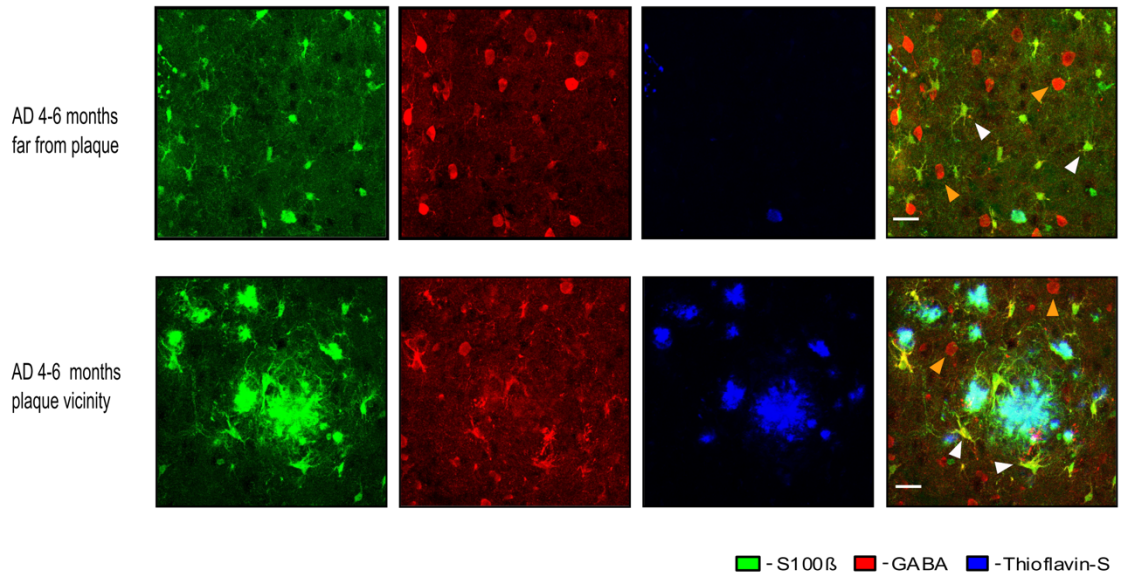

Figure 5: Cortical astrocytes of amyloid-depositing mice at 6 months of age show significant GABA reactivity in the vicinity of amyloid plaques.
Maximum-intensity projection images (4-6 months "far" = 16 slices, 4-6 months "plaque vicinity" = 16 slices) obtained from the frontal cortex in a fixed brain slice of an amyloid-depositing mouse at 6 months of age "far from plaque" (upper row, 16 slices, step size 1 µm) and "plaque vicinity" (lower row, 16 slices, step size 1 µm). Brain slices were labeled with antibodies against S100β (green; left panel), GABA (red; middle panel) and with Thioflavin-S (blue; right panel). In the merged images on the right, S100β-positive astrocytes are indicated by white triangles and GABA-positive interneurons are indicated by orange triangles. Scale bar 20 µm.

Similarly, we were not able to differentiate between astrocytes that are located close and far from plaque in the DG, due to the high plaque load in this area.

Colocalization of GABA and S100β was evident in images showing astrocytes in "plaque vicinity" (Fig. 5 upper row), no colocalization was seen in astrocytes „far from plaque" (Fig. 5 lower row).

An increase in both astrocytic soma size (Fig. 6A and B, left panels) and GABA content (Fig. 6A and B, right panels) occurred only in cells located in „plaque vicinity" compared to astrocytes located „far from plaque" (Fig. 6A; $p<0.01$* for "soma size" and $p<0.01$* for "normalized GABA Intensity"; Student's T-test; Fig 6B; $p<0.01$* for "soma size" and $p<0.01$* for "normalized GABA Intensity"; Kolmogorov-Smirnov-Test).

Furthermore, soma size and GABA content of cells located "far from plaque" were comparable to values of WT mice at the same age (Fig. 6B; soma size: $p = 0.691$; GABA content: $p = 0.176$; Kolmogorov-Smirnov-Test).

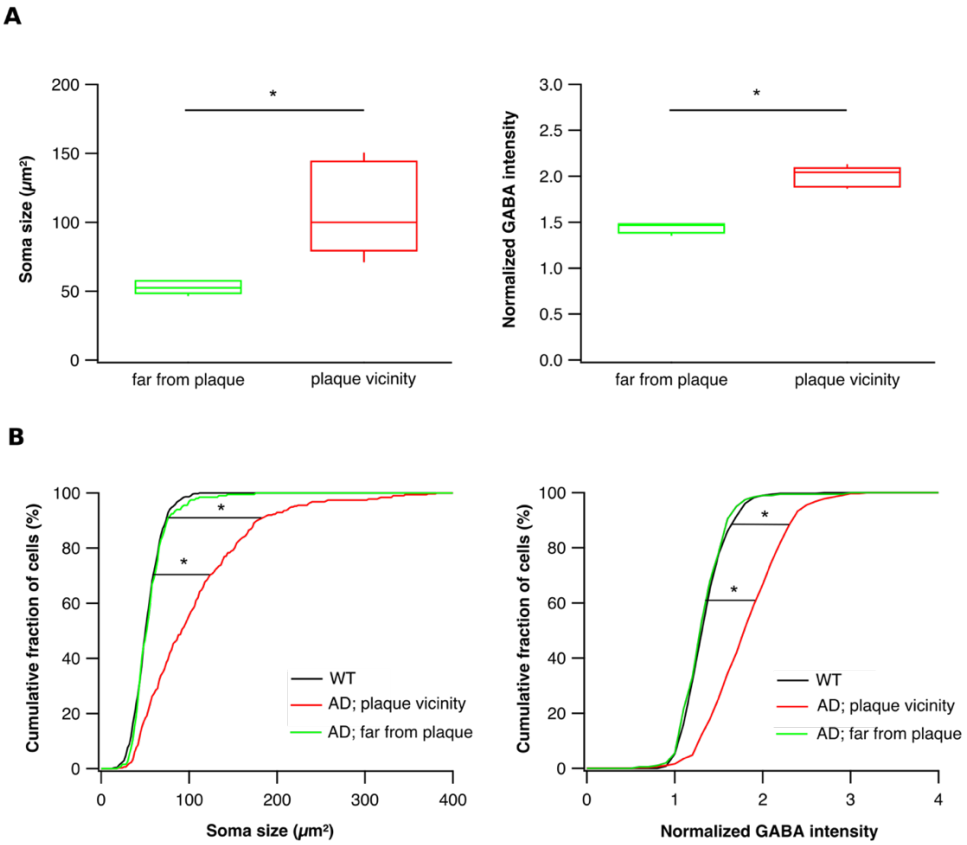

Figure 6: Cortical astrocytes located in "plaque vicinity" show a significant difference in soma size and normalized GABA intensity compared to astrocytes located "far from plaque" at 4-6 months of age. This figure was reproduced from Brawek et al. (2018) [46].
A: Box-and-whisker plots showing median soma size (left; n=5 mice) and normalized GABA intensity (right; n=5 mice) of cortical astrocytes in amyloid-depositing mice at 4-6 months of age, separated into astrocytes located "far from plaque" (green) and in "plaque vicinity" (red). Significant differences were visible for both parameters ($p<0.01$* for "soma size" and $p<0.01$* for "normalized GABA Intensity"; Student's T-test).
B: Distributions of soma size (left) and normalized GABA intensity (right) of cortical astrocytes in amyloid-depositing and WT mice at 4-6 months of age, displayed as cumulative probability histograms. Astrocytes of amyloid-depositing mice were separated into astrocytes located "far from plaque" (green; 200 cells) and astrocytes located in "plaque vicinity" (red; 313 cells). While astrocytes located "far from plaque" showed no difference in soma size and normalized GABA intensity values compared to WT astrocytes ($p=0.176$ for "normalized GABA intensity" and $p=0.691$ for "soma size"; Kolmogorov-Smirnov-Test), astrocytes located in "plaque vicinity" showed a significant difference in both parameters compared to astrocytes in WT mice ($p<0.01$* for all comparisons; Kolmogorov-Smirnov-Test).

Furthermore, there was a positive correlation between the two parameters at 4-6 months of age both in the cortex as well as in the DG (Fig. 7; $r_S=0.51$, $p<0.0001$ in the cortex; $r_S=0.16$, $p=0.021$ in the hippocampus; Spearman correlation), while there was no correlation in the 9-11 months age group neither for cortical nor for

hippocampal astrocytes (Fig 7; r_S=0.014, p=0.842 in the cortex; r_S=0.066, p=0.364 in the DG; Spearman correlation).

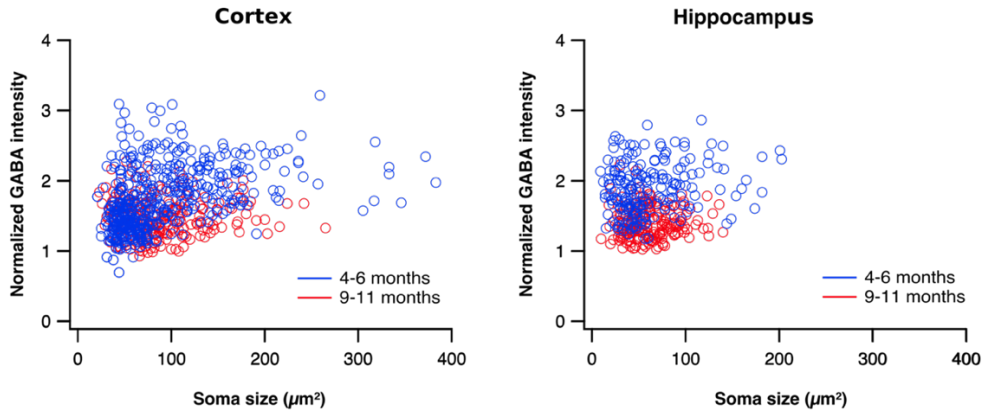

Figure 7: Normalized GABA content is correlated with soma size only in 4-6 months-old amyloid depositing mice. This figure was reproduced from Brawek et al. (2018) [46].
Scatter plots showing astrocytic GABA content as a function of soma size in the cortex (left) and in the hippocampus (right) of 4-6 months (blue; n=5 mice) and 9-11 months old (red; n=5 mice) amyloid-depositing mice. At 4-6 months of age, there was a positive correlation between soma size and GABA content (r_S=0.51, p<0.0001 in the cortex; r_S=0.16, p=0.021 in the hippocampus; Spearman correlation). In 9-11 months old mice, these parameters were not correlated (r_S=0.014, p=0.842 in the cortex; r_S=0.066, p=0.364 in the hippocampus; Spearman correlation).

This leads to the assumption that the processes causing astrocytic hypertrophy and GABA accumulation have a common trigger during the early stages of amyloidosis, while at 9-11 months, when plaques are vastly abundant throughout the cortex, they are governed by different processes.

3.4 Astrocytic GABA content in the course of healthy aging

After we found GABA reactivity in different brain areas of amyloid-depositing mice, we wondered whether this process also occurs in normally aging WT mice. So, we analyzed astrocytes in 1-2, 4-6, 9-11 and 18-20 months old WT mice in the cortex and in the DG.
Images from the DG showed only modest colocalization of S100β and GABA reactivity in all age groups examined (Fig. 8).

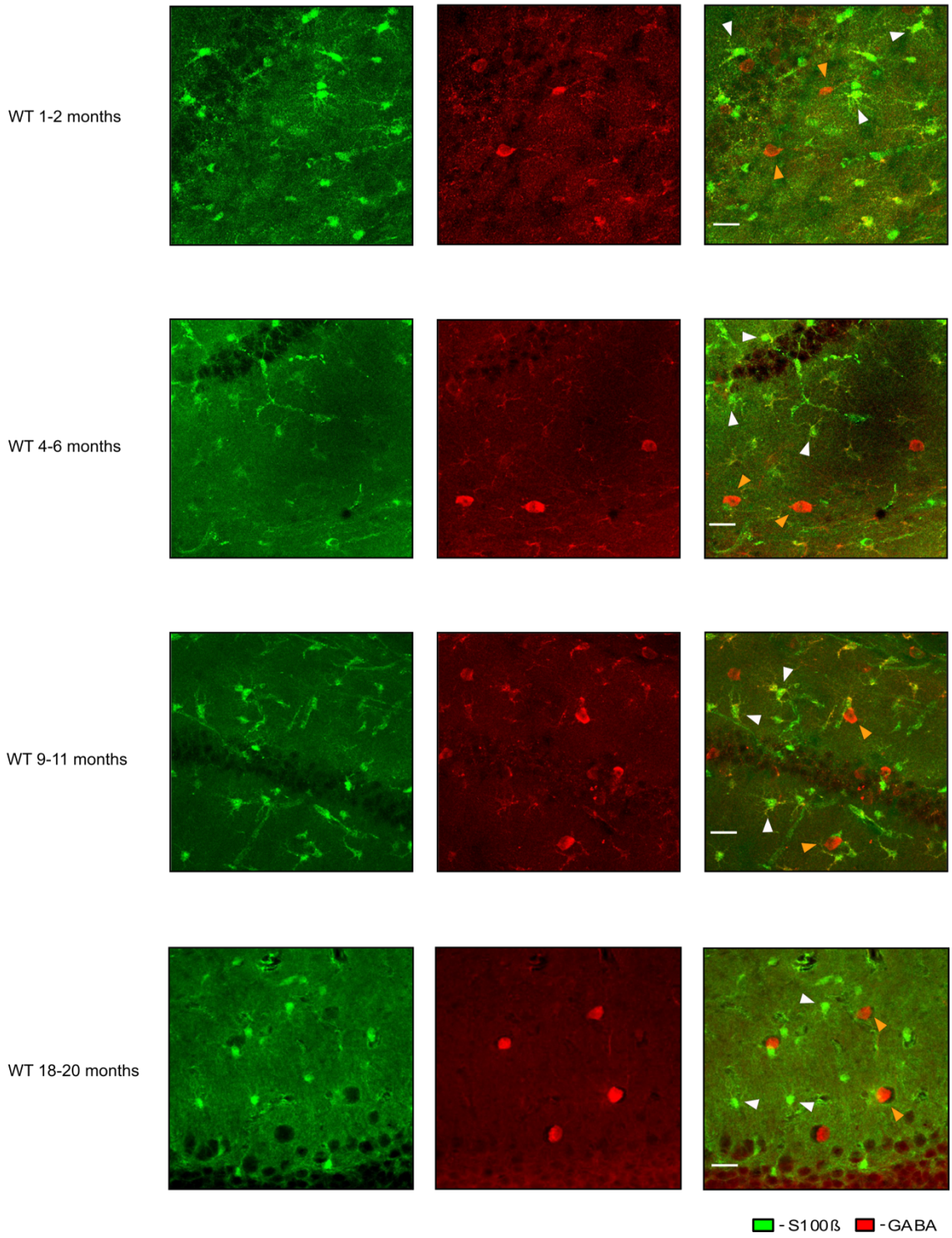

Figure 8: Hippocampal astrocytes of WT mice show little GABA reactivity.
Maximum-intensity protection images obtained from the hippocampus (DG) in a fixed brain slice of an WT mouse at 2 months (first row, 13 slices, step size 1 µm), 5 months (second row, 7 slices, step size 1 µm), 11 months (third row, 16 slices, step size 1 µm) and 19 months (bottom row, 14 slices, step size 1 µm) of age, respectively. Brain slices were labeled with antibodies against S100β (green; left panel) and GABA (red; middle panel). In the merged images on the right, S100β-positive astrocytes are indicated by white triangles and GABA-positive interneurons are indicated by orange triangles. Scale bar 20 µm.

Similar data were obtained in the frontal cortex (Fig. 9).

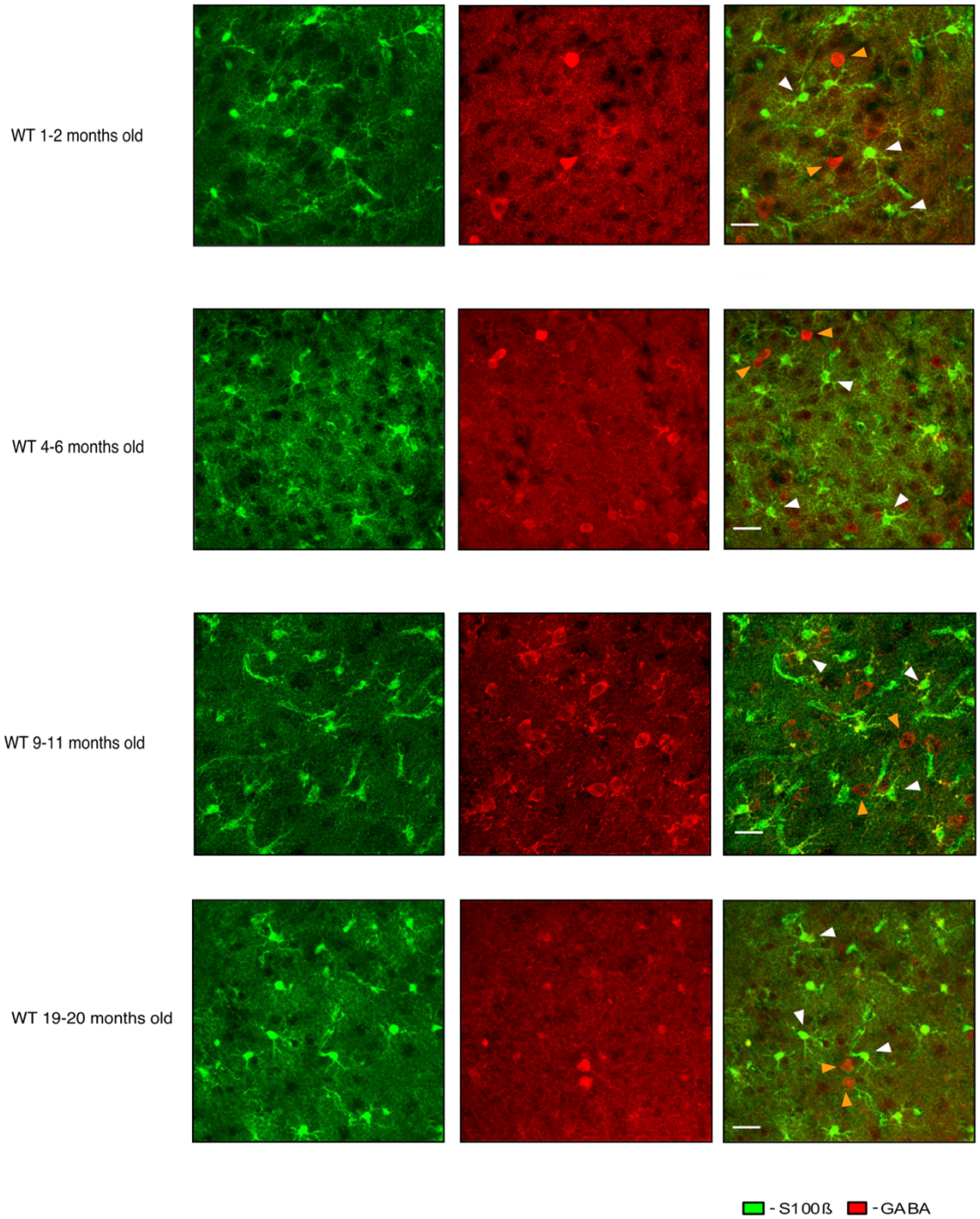

Figure 9: Cortical astrocytes in WT mice show little GABA reactivity.
Maximum-intensity projection images obtained from the frontal cortex in a fixed brain slice of an WT mouse at 2 months (first row, 19 slices, step size 1 µm), 5 months (second row, 21 slices, step size 1 µm), 9 months (third row, 12 slices, step size 1 µm) and 19 months (bottom row, 12 slices, step size 1 µm) of age, respectively. Brain slices were labeled with antibodies against S100β (green; left panel) and GABA (red; middle panel). In the merged images on the right, S100β-positive astrocytes are indicated by white triangles and GABA-positive interneurons are indicated by orange triangles. Scale bar 20 µm.

Comparing astrocytic soma size between the two brain structures, cortical astrocytes were significantly larger than hippocampal astrocytes in all age groups ($p = 0.0001$ for 1-2 months; $p = 0.0007$ for 4-6 months; $p = 0.006$ for 9-11 months; Student's t-test), except for astrocytes in 18-20 months old mice ($p=0.83$; Student's t-test).

In the DG, median astrocytic soma size at 18-20 months of age was significantly larger than in all other age groups (Fig. 10A, left panel; $p = 0.001$; 18-20 months vs. 1-2 months, 4-6 months, and 9-11 months: $p < 0.001$ for all comparisons; one-way ANOVA followed by post-hoc Bonferroni correction for multiple comparisons).

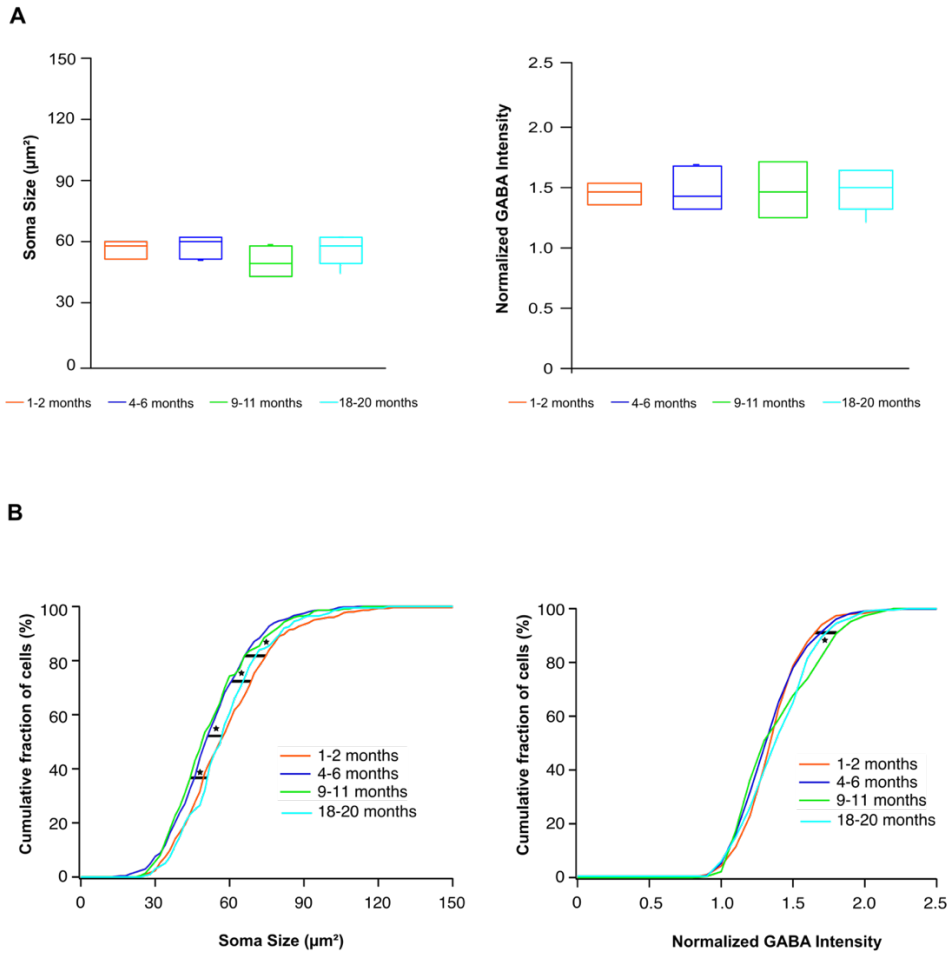

Figure 10: Cortical astrocytes in WT mice show minor differences in GABA content and soma size in the course of aging. This figure was reproduced from Brawek et al. (2018) [46].
A: Box-and-whisker plots showing median soma size (left) and normalized GABA intensity (right) of cortical astrocytes in WT mice at 1-2 months (red; n=5 mice), 4-6 months (blue; n=5 mice), 9-11 months (green; n=5 mice) and 18-20 months (light blue; n=5 mice) of age. There was no change of both parameters during the aging process (p=0.155 for "soma size" and p=0.919 for "normalized GABA intensity"; one-way ANOVA).
B: Distributions of soma size (left) and normalized GABA intensity (right) of cortical astrocytes in WT mice at 1-2 months (red; n=301 cells), 4-6 months (blue; n=514 cells), 9-11 months (green; n=226 cells) and 18-20 months (light blue; n= 200 cells) of age, displayed as cumulative probability histograms. Comparing different age groups, distribution of soma size in 1-2 months and 18-20 months old mice were significantly shifted to the right when compared to that of 4-6 or 9-11 months old mice ($p < 0.01$ for all comparisons, Kolmogorov-Smirnov test), while distribution of GABA intensity was significantly higher in 9-11 months old mice compared to 1-2 months old mice ($p = 0.004$, Kolmogorov-Smirnov test; $p > 0.01$ for all other comparisons). Astrocytes in 18-20 months old mice were not significantly different from all other age groups ($p > 0.01$ for all comparisons, Kolmogorov-Smirnov test).

On the other hand, median soma size of cortical astrocytes did not increase during the course of aging (Fig. 11A, left panel; p= 0.27; one-way ANOVA).

Aging did not significantly increase median astrocytic GABA levels in both cortical and hippocampal astrocytes (Fig. 10A and Fig 11A, right panels; in the cortex: $p = 0.98$; in the DG: 16, $p = 0.14$; one-way ANOVA). However, the normalized GABA intensity was significantly lower in hippocampal than in cortical astrocytes (1-2 months: $p = 0.04$; 4-6 months: $p = 0.03$; 18-20 months: $p = 0.0004$; Student's t-test) except for astrocytes at 9-11 months of age ($p = 0.195$; Student's t-test).

A comparison of the different age groups on the population level (Fig. 10B and 11B, left panels) showed that astrocytic soma size increased with age in the DG, again strikingly in the 18-20 months age group ($p < 0.001$ for comparisons to all other age groups; Kolmogorov-Smirnov test), whereas cortical astrocytes in 4-6 months and 9-11 months old mice showed slightly but significantly smaller soma size than at 1-2 months and 18-20 months of age ($p < 0.01$; Kolmogorov-Smirnov test).

The GABA content increased with age in both cortex and hippocampus (1-2 months vs 9-11 months; in the cortex: $p = 0.004$; in the DG: $p < 0.001$; Kolmogorov-Smirnov test) but returned to lower values in 18-20 months old mice.

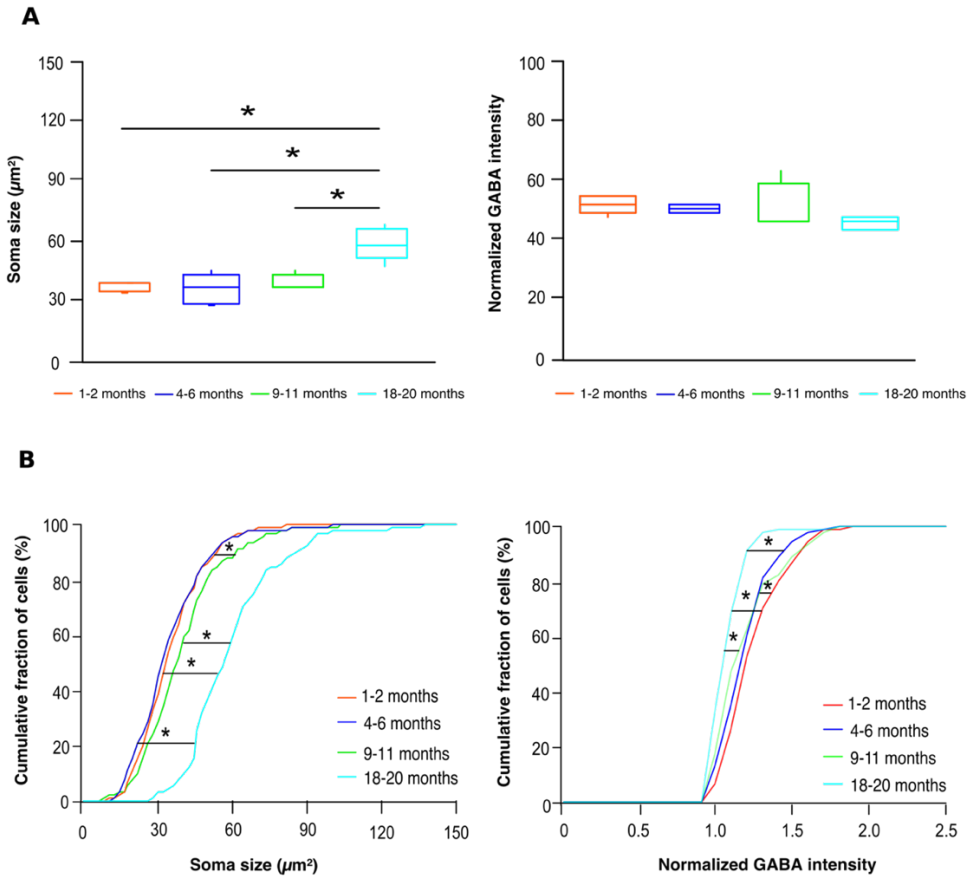

Figure 11: Significant changes in soma size in hippocampal astrocytes of WT mice in the course of aging. This figure was reproduced from Brawek et al. (2018) [46].
A: Box-and-whisker plots showing median soma size (left) and normalized GABA intensity (right) of hippocampal astrocytes in WT mice at 1-2 months (red; n=5 mice), 4-6 months (dark blue; n=5 mice), 9-11 months (green; n=5 mice) and 18-20 months (light blue; n=5 mice) of age. Soma size increased significantly in 18-20 months old animals in comparison to all other age groups ($p = 0.001$; one-way ANOVA; 18-20 months old animals compared to 1-2, 4-6, and 9-11 months old animals: $p < 0.001$ for all comparisons; comparisons between 1-2, 4-6, and 9-11 months old animals: $p = 1$ for all comparisons; post-hoc Bonferroni correction for multiple comparisons) whereas GABA levels were similar ($p = 0.14$, one-way ANOVA).
B: Distributions of soma size (left) and normalized GABA intensity (right) of hippocampal astrocytes in WT mice at 1-2 months (red; n=200 cells), 4-6 months (dark blue; n=195 cells), 9-11 months (green; n= 199 cells) and 19-20 months (light blue; n= 200 cells) of age, displayed as cumulative probability histograms. A significant shift to the right in 9-11 months old mice was visible compared to 4-6 months old mice ($p = 0.004$, Kolmogorov-Smirnov test), whereas there is no difference between 1-2- and 4-6-months old mice and 1-2 and 9-11 months old mice ($p > 0.01$ for both comparisons, Kolmogorov-Smirnov test). In 18-20 months old mice, this shift was even more prominent ($p < 0.001$ for all comparisons, Kolmogorov-Smirnov test). Small differences between 1-2 months and 9-11 months ($p<0,01$* for “Normalized GABA intensity“; Kolmogorov-Smirnov-test) and 4-6 months and 9-11 months ($p<0,01$* for “soma size“; Kolmogorov-Smirnov-test) could be found. Distribution of the normalized GABA intensity was significantly shifted to the left in 18- 20 months old animals compared to all other age groups ($p < 0.001$ for all comparisons, Kolmogorov-Smirnov test).

These results suggest that in healthy mouse brains there is a moderate GABA accumulation in astrocytes during adolescence in healthy mouse brains. Since age dependent changes in soma size and GABA content did not exhibit the same trend in cortex and DG, it's more likely that they are not caused by the identical mechanisms.

3.5 Age-dependent differences between WT and AD mice in cortex and hippocampus

We also compared soma size and GABA content of AD and WT mice directly between the respective age groups and found that there are significant differences in both parameters during the course of aging.
In the cortex of 4-6 months old mice, there was a significant increase in astrocytic soma size in astrocytes located in "plaque vicinity" compared to astrocytes from age-matched WT mice (Fig. 12A, middle panel; $p<0.01$*; Kolmogorov-Smirnov-Test). Astrocytic soma size was also significantly increased in AD mice at 9-11 months of age compared to respective astrocytes in WT mice (Fig. 12A, right panel; $p<0.01$*; Kolmogorov-Smirnov-Test).

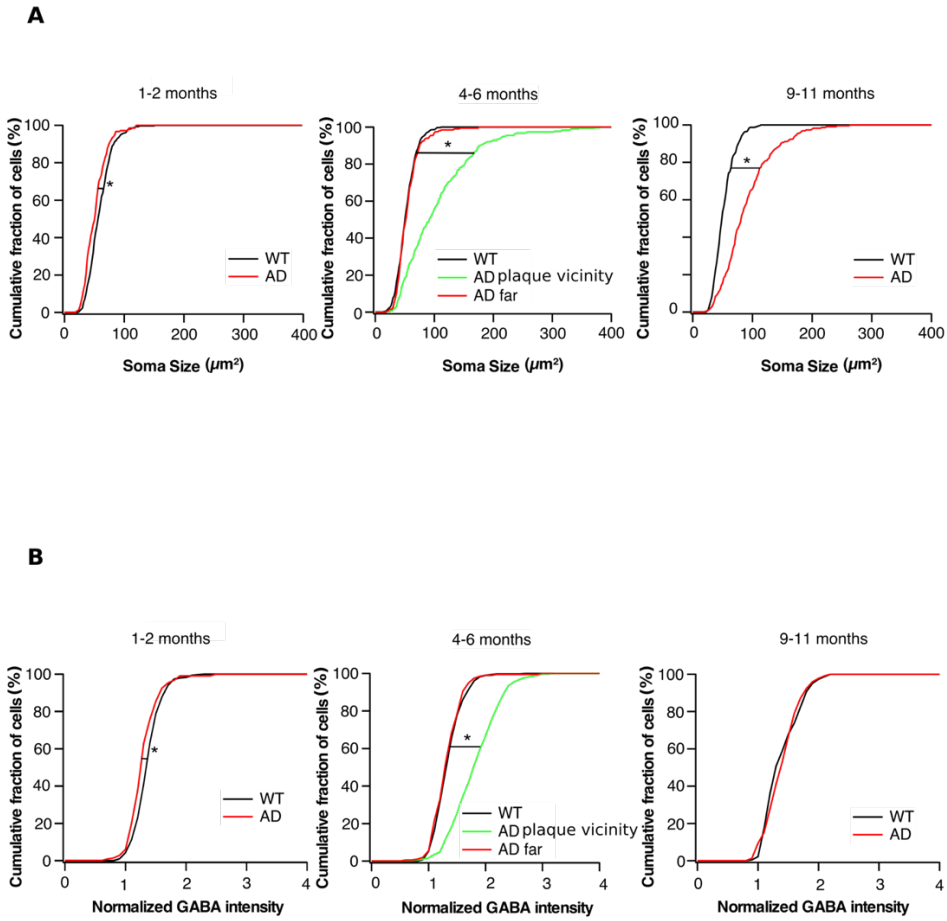

Figure 12: Cortical astrocytes in AD mice show age-dependent differences in soma size and GABA content compared to that of WT mice.

A: Distribution of soma size of cortical astrocytes at 1-2 months (left), 4-6 months (middle) and 9-11 months (right) of age, respectively, displayed as cumulative probability histograms. Astrocytes of AD mice (red; n= 213 cells 1-2 months, n= 513 cells 4-6 months, n= 225 cells 9-11 months) were compared to astrocytes of WT mice (black; n= 301 cells 1-2 months, n=514 cells 4-6 months, n= 226 cells 9-11 months) at the respective age. In the 4-6 months age group there was a significant difference in soma size between astrocytes located in "plaque vicinity" (green; n= 313 cells) and astrocytes located "far from plaque" (red; n=200 cells; $p<0.01$*; Kolmogorov-Smirnov-Test), whereas astrocytes located "far from plaque" had the same size as astrocytes of WT mice ($p=0.691$; Kolmogorov-Smirnov-Test). Also, there was a significant difference in soma size in the 9-11 months age group ($p<0.01$*; Kolmogorov-Smirnov-Test) and a small but significant difference in the 1-2 months age group between astrocytes of AD mice and WT mice ($p< 0.01$*; Kolmogorov-Smirnov-Test).

B: Distributions of normalized GABA intensity of cortical astrocytes at 1-2 months (left), 4-6 months (middle) and 9-11 months (right) of age, respectively, displayed as cumulative probability histograms. Astrocytes of AD mice (red; n= 213 cells 1-2 months, n= 513 cells 4-6 months, n= 225 cells 9-11 months) were compared to astrocytes of WT mice (black; n= 301 cells 1-2 months, n=514 cells 4-6 months, n= 226 cells 9-11 months) at the respective age. Astrocytes of AD mice at 4-6 months of age located in "plaque vicinity" (green; n= 313 cells) had a higher normalized GABA intensity than astrocytes located "far from plaque" (red; n=200 cells; $p<0.01$*; Kolmogorov-Smirnov-Test) and astrocytes of WT mice ($p<0.01$*; Kolmogorov-Smirnov-Test).

For normalized GABA intensity, there was a significant shift in GABA levels in astrocytes located in “plaque vicinity” in AD mice compared to astrocytes of WT mice at 4-6 months of age (Fig. 12B, middle panel; p<0.01*; Kolmogorov-Smirnov-Test).

Additionally, median astrocytic GABA levels at 9-11 months in AD mice showed no difference to GABA levels in WT mice at the same age (Fig. 13, lower row; p = 0.74; Student’s t-test;).

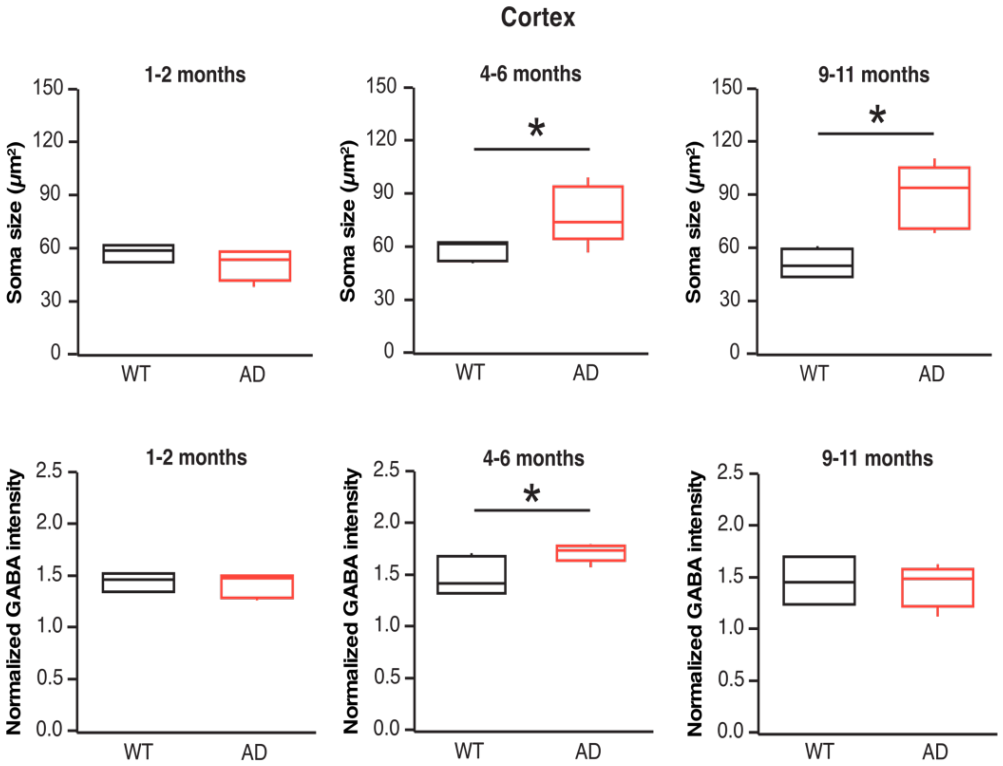

Figure 13: Cortical astrocytes of AD and WT mice show differences in soma size and GABA content in the cortex. This figure was reproduced from Brawek et al. (2018) [46]. Box-and-whisker plots comparing median soma size (upper panel) and normalized GABA intensity of astrocytes in the cortex of 1-2 months (left panel), 4-6 months (middle panel), and 9-11 months (right panel) old WT (black) and AD (red) mice. Both values were significantly higher in 4-6 months old amyloid depositing mice (soma size: p = 0.03; GABA intensity: p = 0.04; Student’s t-test), while values in 1-2 months old pre-depositing mice were similar (soma size: p = 0.18; GABA intensity: p = 0.69; Student’s t-test). Median soma size was significantly larger in AD mice at 9-11 months of age (p = 0.0009; Student’s t-test), whereas median normalized GABA intensities were similar (p = 0.74; Student’s t-test).

Similar results were found for the hippocampus. Across all ages, there was a significant difference in astrocytic soma size comparing AD and WT mice (Fig. 14A; p<0.01* for all comparisons; Kolmogorov-Smirnov-Test).

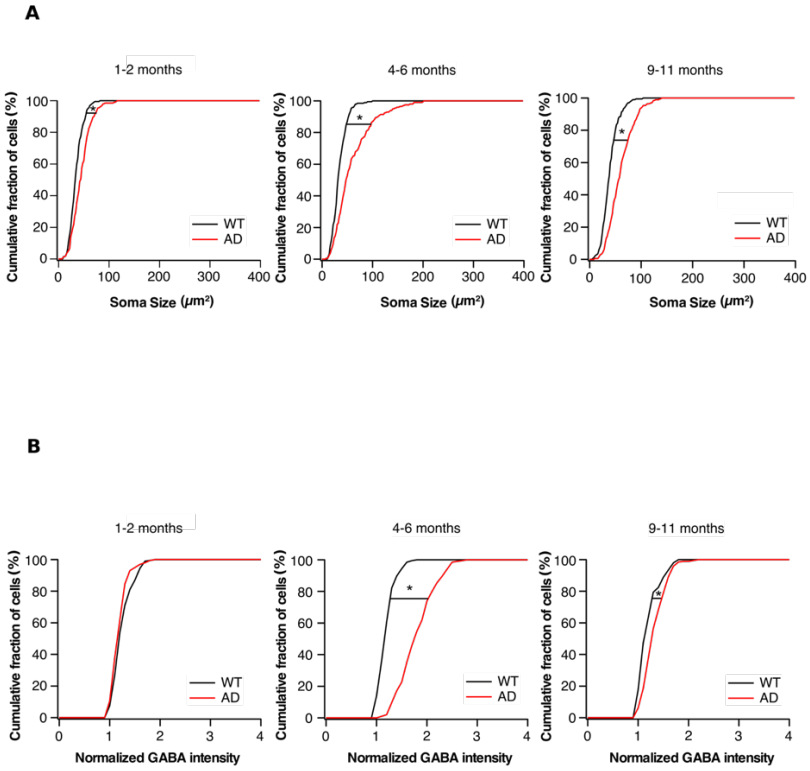

Figure 14: Hippocampal astrocytes in AD mice show age-dependent differences in soma size and GABA content compared to that of WT mice.
A: Distributions of soma size of hippocampal astrocytes at 1-2 months (left), 4-6 months (middle) and 9-11 months (right) of age, respectively, displayed as cumulative probability histograms. Astrocytes of amyloid-depositing mice (red; n= 200 cells 1-2 months, n= 199 cells 4-6 months, n= 195 cells 9-11 months) were compared to astrocytes of WT mice (black; n= 200 cells 1-2 months, n= 195 cells 4-6 months, n= 199 cells 9-11 months) at the respective age. There was a significant difference in soma size between astrocytes of AD mice and astrocytes of WT mice in all age groups (p<0,01*; Kolmogorov-Smirnov-Test); however, the soma size value increased from 1-2 months to 4-6 months and then decreased from 4-6 months to 9-11 months in amyloid-depositing mice.
B: Distributions of normalized GABA intensity of hippocampal astrocytes at 1-2 months (left), 4-6 months (middle) and 9-11 months (right) of age, respectively, displayed as cumulative probability histograms. Astrocytes of AD mice (red; n= 200 cells 1-2 months, n= 199 cells 4-6 months, n= 195 cells 9-11 months) were compared to astrocytes of WT mice (black; n= 200 cells 1-2 months, n= 195 cells 4-6 months, n= 199 cells 9-11 months) at the respective age. There was no significant difference in normalized GABA intensity in the 1-2 months age group between astrocytes of AD mice and astrocytes of WT mice (p=0,027; Kolmogorov-Smirnov-Test), while the difference was significant in both 4-6 months and 9-11 months old mice (p<0,01*; Kolmogorov-Smirnov-Test). Comparing normalized GABA intensity in AD mice in the course of aging, it increased gravely from 1-2 months to 4-6 months and subsequently decreases in 9-11 months old mice.

For GABA intensity, there was a large difference between AD and WT mice at 4-6 months of age (Fig. 14B, middle panel; p<0.01*; Kolmogorov-Smirnov-Test), while there was a small but significant difference comparing astrocytic GABA content in AD and WT mice at 9-11 months of age (Fig. 14B; p<0.01*; Kolmogorov-Smirnov-Test).

Again, median astrocytic GABA levels at 9-11 months in AD mice showed no difference to GABA levels in WT mice of the same age (Fig. 15, lower row; p= 0.38; Student's t-test;).

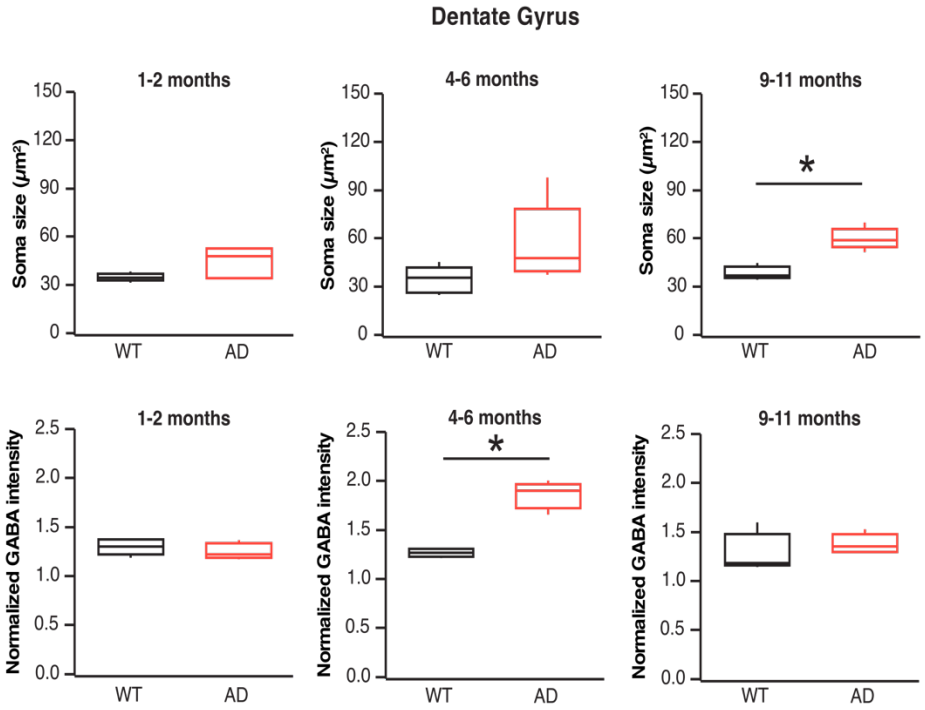

Figure 15: Astrocytes in AD and WT mice show differences in soma size and GABA content in the DG. This figure was reproduced from Brawek et al. (2018) [46]. Box-and-whisker plots comparing median soma size (upper panel) and normalized GABA intensity of astrocytes in the DG of 1-2 months (left panel), 4-6 months (middle panel), and 9- 11 months (right panel) old WT (black) and AD (red) mice. In pre-depositing mice at 1-2 months of age, both parameters were similar (soma size: p = 0.06; GABA intensity: p = 0.38; Student's t-test). Values for soma size were similar in 4-6 months old mice (p = 0.09; Student's t-test), but GABA intensity was higher in AD mice (0 = 0.0001; Student's t-test). Values for soma size were larger mice of 9-11 months of age (p = 0.0006; Student's t-test), while median normalized GABA intensity compared to WT mice was similar (p = 0.38; Student's t-test).

These results provide further evidence for the influence of amyloid formations on astrocytes and also for an up-and-down trend of astrocytic GABA content during the course of the disease.

3.6 GABA reactivity can also be found without the presence of amyloid plaques

Now that we found out that amyloid-depositions have an impact on astrocytic GABA levels and hypertrophy, we wanted to test if GABA accumulation can also appear in the absence of plaques.
To this end, we decided to analyze astrocytes in 4-6 months old PS45 mice (Fig. 16). In PS45 mice, mouse Aβ42 production is increased due to the expression of the AD-associated G384A mutation in PS1, but they do not show signs of inflammation or plaque-deposition. In the frontal cortex of these mice, we could identify moderate GABA accumulation in astrocytes (Fig. 16 lower row).

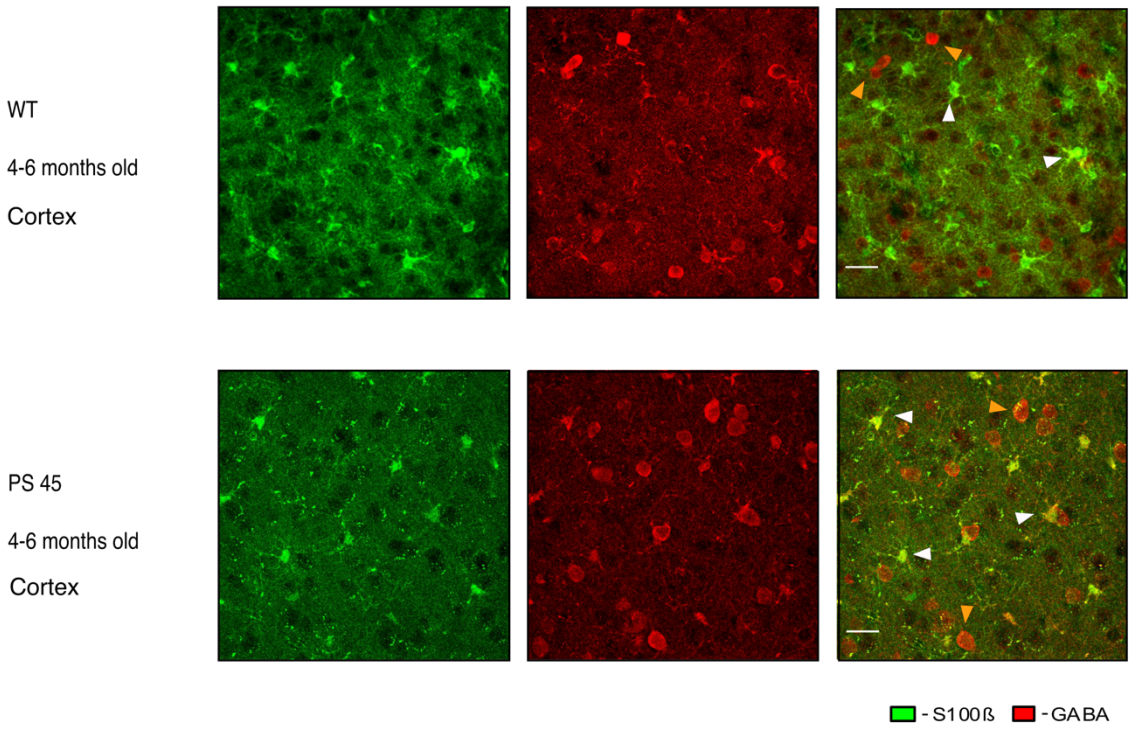

Figure 16: Cortical astrocytes in PS45 mice without amyloid deposition show GABA reactivity.
Maximum-intensity projection images obtained from the frontal cortex in a fixed brain slice of an WT mouse at 5 months of age (upper row, 21 slices, step size 1 µm) and an PS45 mouse at 6 months of age (bottom row, 15 slices, step size 1 µm). Brain slices were labeled with antibodies against S100β (green; left panel) and GABA (red; middle panel). In the merged images on the right, S100β-positive astrocytes are indicated by white triangles. Orange triangles indicate GABAergic interneurons. Scale bar 20 µm.

Comparing median soma size, astrocytes of PS45 mice surprisingly had a significantly smaller median soma size than astrocytes in WT mice at the same age (Fig. 17A, left figure; p= 0.04*, Student's t-test). There was a trend towards higher GABA levels in astrocytes of PS45 mice, however, it did not reach statistical significance (Fig. 17B, right panel; p= 0.11, Student's t-test).
Comparing the cumulative distributions of soma size and normalized GABA intensity, we found a significant shift in astrocytic GABA levels towards higher values in PS45 mice compared to WT mice (Fig. 17B, right panel; p<0.01*, Kolmogorov-Smirnov test), yet soma size was similar (Fig. 17B, left panel; p= 0.104, Kolmogorov-Smirnov test).
In both PS45 mice and WT mice, astrocytic soma size and GABA intensity were negatively correlated (Fig. 17C, Spearman's rank correlation coefficient for WT

mice r_s =-0.237, p < 0.0001, for PS45 mice r_s=-0.2551, p = 0.0001), leading to the assumption that, in this case, smaller astrocytes accumulate more GABA.

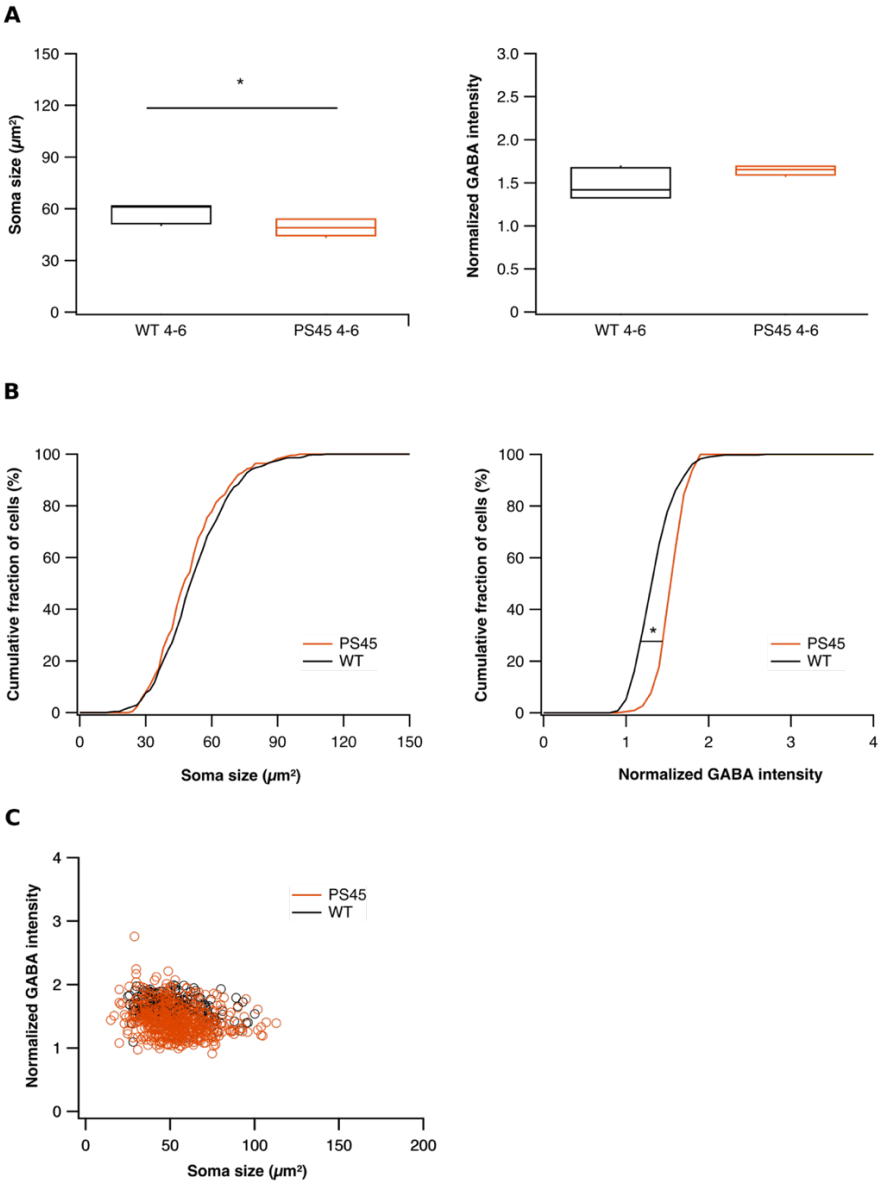

Figure 17: Cortical astrocytes in PS45 mice show a difference in normalized GABA intensity, but no increase in soma size. This figure was reproduced from Brawek et al. (2018) [46].
A: Box-and-whisker plots showing median soma size (left) and normalized GABA intensity (right) of cortical astrocytes in WT mice (black, n=5 mice) and PS45 mice (orange; n=5 mice) at 4-6 months of age. There was a slight but significant difference in soma size (p= 0.04'; Student's T-Test), but none in normalized GABA intensity (p= 0.156539; Student's T-Test).
B: Distribution of soma size (left) and normalized GABA intensity (right) of cortical astrocytes in WT mice (black; n= 195 cells) and PS45 mice (orange; n= 228 cells) at 4-6 months of age, displayed as cumulative probability histograms. While there was a significant difference in normalized GABA intensity between astrocytes in PS45 and WT mice (p<0.01*, Kolmogorov-Smirnov-Test), there was no difference in soma size.

C: Scatter plots showing astrocytic GABA content as a function of soma size in the cortex of WT (black) and PS45 mutant mice (orange) at 4-6 months of age. There was a negative correlation between soma size and GABA intensity in both WT as well as PS45 mice (r_S= - 0.2551, p<0.0001 for PS 45 mice; Spearman correlation).

These results show that an increase in astrocytic GABA content can also occur in the absence of amyloid plaques due to AD-related mutations in PS1 and that astrocytic hypertrophy and GABA content are controlled by different mechanisms.

4. Discussion

Here, we studied two parameters of astrocytes known to be affected in the course of amyloidosis, soma size and GABA content. These parameters were studied in the cortex and hippocampal DG during plaque deposition in a mouse model of AD as well as during normal aging in WT mice.

Three different key observations were made:

1. Moderate but significant alterations in GABA content and soma size of astrocytes can be found during the normal aging process in the cortex and DG.
2. Astrocytes in amyloid-depositing mice exhibit a bell-shaped dependence of GABA content on age during the course of amyloidosis in both cortex and DG, while astrocytic soma size continuously increases.
3. Mice with a mutation in the PS1 gene devoid of amyloid plaque development show elevated astrocytic GABA content.

It is well known that astrocytes exhibit distinct alterations in phenotype and function during the course of healthy aging [47-53]. As previously reported similarly for astrocytes in the hippocampal DG of 24-months old WT mice [47], we observed a small but significant increase in astrocytic soma size in mice 9-11 months old mice, also in the DG. This increase becomes even more apparent at 18-20 months old mice. Hence this leads to the assumption that an increase in soma size caused by the aging process begins during late adulthood and becomes even more apparent in the course of aging.
Cortical astrocytes, however, exhibit minor alterations during aging with significant hypertrophy in aged mice after a decrease of soma size in early adulthood.
Since we found an increase in astrocytic soma size in both the DG and cortex in aged mice compared to adult animals, this suggests that a hypertrophy of astrocytes is a byproduct of the aging-related moderate proinflammatory condition known to be present in the senescent brain [48-50].

The effect of aging on astrocytic phenotype and function is still unclear. Rodriguez et al. (2014) proposed that S100β, a Ca^{2+}-binding protein expressed in astrocytes and presumably responsible for different types of neuro-glial interactions, may play a role [47]. Possibly S100β impairs cognition, and elevated levels of S100β were measured in the blood of aged humans affected with affected cognitive function. This assumption, however, needs additional confirmation [47]. An increase in soma size was also measured in astrocytes in the DG and entorhinal cortex (EC) of 24 old WT mice, however, no connection to an increase in astrocytic GABA content was made [47].

Grosche et al. (2013) studied morphological changes caused by the aging process in astrocytes in the hippocampus and cortex. They compared territories, covered by individual astrocytes in 5 months old and 21 months old WT mice and found an increase in territorial volume in cortical astrocytes and doubled territorial volume in hippocampal astrocytes [54].

They proposed that this increase in territorial volume is caused by increased oxidative stress in the aging brain. Astrocytes, who are the predominant cells to prohibit oxidative stress in the brain and maintain this role also in senescent animals, possibly enlarge their domains to successfully clear reactive oxygen species that pile up as the brain ages.

Although they did not report any alteration in soma size, it seems likely that soma size also increases with astrocytic territories during aging, which would fit to our data. An increase in astrocytic territory could also mean that more neurons and other cells like microglia can be contacted by astrocytes, thereby influencing network activity or the inflammatory response in the aging brain.

Surprisingly, median soma size was larger in cortical astrocytes in all age groups studied when compared to astrocytes in the DG (except for 18-20 months old mice), providing further evidence for the regional variability of astrocytes which includes differences in morphological structure as well as physiological functions [51, 52].

Astrocytic GABA content also exhibited modest but significant alterations during the course of normal aging. In the DG, the most obvious alteration was a significant increase in soma size in 18-20 months old mice compared to all other

age groups. In cortical astrocytes, however, no such prominent alteration was observed.

A possible reason for this varying behavior of astrocytes in the cortex and hippocampus may be the different influence of network activities on astrocytes. Astrocytes are able to release neurotransmitters like GABA and glutamate. Since the release of these neurotransmitters can trigger small inward or outward currents when released [17, 18, 55], it is possible to assume that neurotransmitters released by astrocytes play an important role in maintaining neuronal network activity.

In our AD mouse model, we see a gradual increase of soma size and plaque development in the cortex and hippocampus, with a peak soma size at the stage of severe amyloidosis (9-11 months), suggesting that amyloid deposition per se or associated factors are responsible for hypertrophy. Surprisingly, astrocytic GABA content did not increase continuously with age. At 4-6 months of age, the starting phase of plaque formation, we measured surprisingly high astrocytic GABA values in the cortex and hippocampus. At 4-6 months of age in the cortex we found hypertrophic astrocytes with high GABA levels exclusively in the vicinity of amyloid plaques (closer than 60 µm), while astrocytes further away than 60 µm from the nearest amyloid plaque exhibited GABA levels and soma sizes comparable to those of WT mice. This leads to the assumption that at the beginning of AD, accumulation of GABA in astrocytes and astrocytic hypertrophy are caused by amyloid plaque formations. Both parameters were highly correlated at 4-6 months of age, supporting this theory.

At 9-11 months of age, at the stage of the disease where plaques are vastly abundant throughout the brain, soma size continues to increase. In contrast, astrocytic GABA content did not follow this expected pattern but returned to GABA levels comparable to those before plaque deposition, both in the cortex and hippocampus. Additionally, soma size and GABA content were not correlated anymore in 9-11 months old mice. These observations indicate that astrocytic hypertrophy and accumulation of GABA are both triggered by the emergence of amyloid plaques but are actually two separate processes that take a different

development in the course of the disease. In fact, amyloid depositions do not further increase GABA in astrocytes as the disease progresses.

Previous studies on astrocytic GABA accumulation in mouse models of AD only studied a specific age range and were therefore not able to uncover the bell-shaped profile we see here [16, 20]. Additionally, they used different models of AD, which differ in the kinetics and severity of amyloidosis [16, 20].

Wu et al. (2014) studied 5xFAD mice, in which development of pathology is comparable to our APP23xPS45 mouse model [11, 22, 56, 57]. Therefore, it is not surprising that they also report high astrocytic GABA levels at the age they studied (6-8 months), corresponding to the starting phase of plaque deposition. Jo et al. (2014), in contrast, observed elevated GABA levels in older mice at an age of 8- 13 months [16, 20]. However, as they used a different mouse strain (APPswe/PSEN1dE9) mice with a delayed and moderate plaque deposition [11], this age range probably similarly catches the beginning of amyloid pathology and the results are therefore not contradicting our own observations.

The reason for the decrease in astrocytic GABA levels, which we found at later stages of the disease and the ensuing effects on neurons remains elusive. We suppose that astrocytic GABA accumulation and the associated release of GABA are ways to adapt to and to counteract neuronal hyperactivity, which is a known phenomenon associated with amyloid plaques already early during disease progression [22, 28, 29, 31, 58].

Busche et al. (2008,2012) point out that neurons in both the cortex and hippocampus show hyperactivity in the vicinity of amyloid plaques [22, 29].

The exact distance that separated hyperactive from normal or silent neurons was 60 µm from the border of an amyloid plaque, which is the same distance that separated hypertrophic, reactive astrocytes from normal astrocytes in Jo et al. (2014) [20], and also the same distance we found that separates high-GABA astrocytes from low-GABA astrocytes, which further supports the hypothesis that astrocytic GABA accumulation could be a direct response to pathological network activity.

However, it is surprising that we did not observe a constant increase in astrocytic GABA content along with the constant increase in amyloid depositions.

Furthermore, the mouse models used by Jo et al. (APPswe/PSEN1dE9) and Wu et al. (5xFAD) are also known to exhibit neuronal hyperactivity[57, 58]. The fact that these groups found GABA-reactivity of astrocytes in AD mouse models that also show disturbances in neuronal network can be a further sign that during the course of AD, astrocytes turn reactive to counterbalance the beginning of neuronal hyperactivity but are getting exhausted as the disease, as well as the severity of neuronal hyperactivity, progresses.

Consistently, we also found GABA-positive astrocytes in PS45 mice, a mouse line devoid of amyloid depositions but with disturbances in the neuronal network [32], which are comparable to those found in AD mice.

Lerdkrai et al (2018) found that during the aging process in both AD and WT mice, neuronal activity of cortical neurons is also enhanced, which could also be accompanied by elevated astrocytic GABA levels [32].

Based on these observations one can argue astrocytes reach two different functional stages in the course of AD: “fighting” astrocytes (increased GABA levels, large cell soma), appearing at the onset of amyloid deposition and the beginning of neuronal hyperactivity, and “frustrated” astrocytes (decrease in GABA content, large cell soma), appearing when plaques are vastly abundant throughout the brain. It can be argued that, although to a significantly lesser degree, astrocytes go through the same aforementioned development during normal aging, reaching a “frustrated” stage in the advanced aging process after a “fighting” state during late adulthood.

Conclusion:

To sum up, we have shown that astrocytes accumulate GABA in the presence of amyloid depositions, in the early phase of healthy aging and as a reaction to AD-associated mutation of PS1 in the absence of plaques. At the beginning of plaque formation, the initial cause for astrocytic GABA content and hypertrophy is likely the same, namely amyloid plaques or factors directly associated with them, for example oligomers that surround amyloid plaques or inflammatory factors. The reason for the increase in soma size might be an immune response, while hyperactivity of neurons may be the reason for elevated GABA levels. We assume that the elevated intracellular astrocytic GABA levels and GABA release as well as an ensuing tonic inhibition [16, 20] are defense-mechanisms of the brain trying to prevent neuronal hyperactivity caused by amyloid plaques or AD-associated mutations of PS1. Therefore, it might be counterproductive to lower GABA levels with pharmacotherapy for AD patients, since it would impede the aforementioned defense mechanism and disturbances in neuronal network activity could possible occur at a faster rate. This approach would also prove to be ineffective over time, since there is a decrease in astrocytic GABA content in the advanced phases of the disease. A more promising way of treating AD seems to be the regulation of intracellular Ca^{2+}-stores [32, 59] or inhibition of other mechanisms causing neuronal hyperactivity [60, 61] and therefore the prevention of neuronal network disturbances right when they start.

5. Abstract

Alzheimer's disease (AD) is the most frequent form of dementia. Mutations in the genes for the amyloid precursor protein (APP) or presenilin 1 (PS1) and presenilin 2 (PS2) respectively, are mostly responsible for the onset of familiar forms of AD. In mouse models of AD, connections between the appearance of amyloid formations and disturbances of neuronal network function have been seen. Consequences of these disturbances are, amongst others, a change in the ratio of hypoactive and hyperactive neurons in the hippocampus and cortex [22, 29]. GABA release by reactive astrocytes in the hippocampus has been proposed as a balancing mechanism of the organism to counteract such neuronal hyperactivity [16, 20]. However, it appears that these balancing mechanisms have a negative effect as they lead to memory deficits.

So far, it is unclear whether the GABA accumulation and release by astrocytes in the hippocampus can also be found in other areas of the brain, like the cortex, and how this mechanism changes during progression of the disease.

In this study, we used immunohistochemistry to stain brain slices from AD mice (APP23xPS45) and age-matched wild-type (WT; C57BL/6) mice and determined GABA content and soma size of S100β-positive astrocytes in the cortex and hippocampus in three different age groups (1-2 months, 4-6 months and 9-11 months) of both AD and WT mice.

In the cortex, we found GABA-positive astrocytes only in the presence of amyloid depositions. Surprisingly, however, there was a significant decrease in astrocytic GABA levels as the disease progresses. In fact, GABA levels of astrocytes in 9-11 months old AD mice were comparable to those in age-matched WT mice. This up-and-down trend was similarly present in the hippocampus of AD mice.

Our data suggest that initially GABA accumulation might be caused by plaque deposition as we found GABA positive astrocytes only in the vicinity of plaques in the cortex. The reason for the decrease in astrocytic GABA content at later stages of the disease remains unclear [32, 41].

We suppose that the transient increase in astrocytic GABA content is a protective mechanism to balance neuronal hyperactivity and hyperexcitability. This conclusion is supported by increased astrocytic GABA levels in PS45 and

normally aged mice, in which neuronal hyperactivity can also be found. This protective mechanism, however, only seems to be operative at the beginning of plaque deposition.

This leads to the assumption that astrocytes reach two different stages over the course of the disease: the “fighting“ stage (high GABA levels, increased soma size) as a reaction to the beginning of amyloid deposition at 4-6 months and the “frustrated” stage (increased soma size, low GABA levels) when plaques become ubiquitous.

6. Dt. Zusammenfassung

Morbus Alzheimer ist die häufigste Form der Demenz. Mutationen in den Genen für das Amyloid Vorläufer Protein (APP) oder Präsenilin 1 (PS1) bzw. Präsenilin 2 (PS2) sind größtenteils für die Entstehung der familiären Form der Erkrankung verantwortlich. In Mausmodellen der Alzheimer-Krankheit wurde eine Verbindung zwischen dem Auftauchen von amyloiden Strukturen und Störungen im neuronalen Netzwerk entdeckt. Auswirkungen dieser Störungen sind, unter anderem, eine Veränderung im Verhältnis von hypoaktiven zu hyperaktiven Neuronen in Hippocampus und Kortex [22, 29]. Die Freisetzung von GABA aus reaktiven Astrozyten im Hippocampus ist potentiell eine der ausgleichenden Maßnahmen, um der neuronalen Hyperaktivität entgegenzuwirken [16, 20]. Es scheint jedoch, dass diese ausgleichenden Maßnahmen einen negativen Effekt mit sich bringen, da sie zu Gedächtnisverlust führen könnten. Unklar ist, ob die GABA Aufnahme und Freisetzung durch Astrozyten im Verlauf der Alzheimer-Krankheit auf den Hippocampus beschränkt ist, oder ob diese Prozesse auch in anderen Teilen des Gehirns, beispielsweise im Kortex, stattfinden. Unklar ist außerdem, ob und wie sich die GABA Akkumulation in Astrozyten im Verlauf der Krankheit verändert.

In dieser Studie benutzten wir Immunhistochemie in fixierten Gehirnschnitten von Amyloid-ablagernden Mäusen (APP23xPS45) und gleichaltrigem Wildtyp Mäusen (WT; C57Bl/6). Wir untersuchten die astrozytäre Somagröße, die mit einer Aktivierung von Astrozyten verknüpft ist, parallel zum astrozytären GABA Gehalt im Kortex und Hippocampus in drei verschiedenen Altersgruppen (1-2 Monate, 4-6 Monate und 9-11 Monate). Im Kortex fanden wir GABA-positive Astrozyten lediglich in der Umgebung von amyloiden Ablagerungen. Überaschenderweise jedoch stellten wir einen signifikanten Rückgang des astrozytären GABA Gehalts bei fortschreitender Erkrankung fest. Tatsächlich war der GABA Gehalt von Amyloid-assoziierten Astrozyten aus 9-11 Monate alten AD Mäusen vergleichbar mit dem von gleichaltrigen WT Mäusen. Diese glockenförmige Entwicklung mit fortschreitender Krankheit war im Hippocampus von AD Mäusen ebenfalls zu beobachten.

Unsere Daten legen nahe, dass die GABA Aufnahme anfangs durch Plaque-Ablagerungen verursacht werden könnte, da wir GABA positive Astrozyten nur im Umkreis von Plaques im Kortex und Hippocampus nachweisen konnten. Der Grund für den Rückgang des astrozytären GABA Gehalts in den späteren Phasen der Krankheit bleibt unklar [32, 41]. Wir nehmen an, dass der vorübergehende Zuwachs des astrozytären GABA Gehalts und die assoziierte GABA Freisetzung einen kompensatorischen Schutzmechanismus zum Ausgleich der neuronalen Hyperaktivität darstellt. Diese Vermutung wird durch eine Zunahme des GABA Gehalts in PS45 und normal gealterten Mäusen, bei denen bekannt ist, dass sie ebenfalls neuronale Hyperaktivität entwickeln, unterstützt.

Dies führt zu der Annahme, dass Astrozyten im Verlauf der Krankheit zwei unterschiedliche Funktionszustände annehmen: einen „kämpfenden“ Zustand (großer GABA Gehalt, vergrößertes Soma) als Reaktion auf das Auftreten von amyloiden Strukturen in 4-6 Monate alten Mäusen, und einen „frustrierten“ Zustand (vergrößertes Soma, niedriges GABA Niveau) bei fortgeschrittener Amyloidose.

7. Literature

1. Hall, A.M. and E.D. Roberson, *Mouse models of Alzheimer's disease.* Brain Res Bull, 2012. **88**(1): p. 3-12.
2. Goedert, M. and M.G. Spillantini, *A century of Alzheimer's disease.* Science, 2006. **314**(5800): p. 777-81.
3. Palop, J.J. and L. Mucke, *Amyloid-beta-induced neuronal dysfunction in Alzheimer's disease: from synapses toward neural networks.* Nat Neurosci, 2010. **13**(7): p. 812-8.
4. Palop, J.J. and L. Mucke, *Epilepsy and cognitive impairments in Alzheimer disease.* Arch Neurol, 2009. **66**(4): p. 435-40.
5. Holtzman, D.M., J.C. Morris, and A.M. Goate, *Alzheimer's disease: the challenge of the second century.* Sci Transl Med, 2011. **3**(77): p. 77sr1.
6. Perez-Nievas, B.G. and A. Serrano-Pozo, *Deciphering the Astrocyte Reaction in Alzheimer's Disease.* Front Aging Neurosci, 2018. **10**: p. 114.
7. Thinakaran, G. and E.H. Koo, *Amyloid precursor protein trafficking, processing, and function.* J Biol Chem, 2008. **283**(44): p. 29615-9.
8. Spires-Jones, T.L. and B.T. Hyman, *The intersection of amyloid beta and tau at synapses in Alzheimer's disease.* Neuron, 2014. **82**(4): p. 756-71.
9. O'Brien, R.J. and P.C. Wong, *Amyloid precursor protein processing and Alzheimer's disease.* Annu Rev Neurosci, 2011. **34**: p. 185-204.
10. Guimas Almeida, C., et al., *Impact of late-onset Alzheimer's genetic risk factors on beta-amyloid endocytic production.* Cell Mol Life Sci, 2018. **75**(14): p. 2577-2589.
11. Jankowsky, J.L., et al., *Mutant presenilins specifically elevate the levels of the 42 residue beta-amyloid peptide in vivo: evidence for augmentation of a 42-specific gamma secretase.* Hum Mol Genet, 2004. **13**(2): p. 159-70.
12. Yiannopoulou, K.G. and S.G. Papageorgiou, *Current and future treatments for Alzheimer's disease.* Ther Adv Neurol Disord, 2013. **6**(1): p. 19-33.
13. Sofroniew, M.V. and H.V. Vinters, *Astrocytes: biology and pathology.* Acta Neuropathol, 2010. **119**(1): p. 7-35.
14. Volterra, A. and J. Meldolesi, *Astrocytes, from brain glue to communication elements: the revolution continues.* Nat Rev Neurosci, 2005. **6**(8): p. 626-40.
15. Assefa, B.T., A.K. Gebre, and B.M. Altaye, *Reactive Astrocytes as Drug Target in Alzheimer's Disease.* Biomed Res Int, 2018. **2018**: p. 4160247.
16. Wu, Z., et al., *Tonic inhibition in dentate gyrus impairs long-term potentiation and memory in an Alzheimer's [corrected] disease model.* Nat Commun, 2014. **5**: p. 4159.
17. Agulhon, C., et al., *Calcium Signaling and Gliotransmission in Normal vs. Reactive Astrocytes.* Front Pharmacol, 2012. **3**: p. 139.

18. Nava-Mesa, M.O., et al., *GABAergic neurotransmission and new strategies of neuromodulation to compensate synaptic dysfunction in early stages of Alzheimer's disease.* Front Cell Neurosci, 2014. **8**: p. 167.
19. Palmer, J.C., et al., *Endothelin-converting enzyme-2 is increased in Alzheimer's disease and up-regulated by Abeta.* Am J Pathol, 2009. **175**(1): p. 262-70.
20. Jo, S., et al., *GABA from reactive astrocytes impairs memory in mouse models of Alzheimer's disease.* Nat Med, 2014. **20**(8): p. 886-96.
21. Preston, A.R. and H. Eichenbaum, *Interplay of hippocampus and prefrontal cortex in memory.* Curr Biol, 2013. **23**(17): p. R764-73.
22. Busche, M.A., et al., *Clusters of hyperactive neurons near amyloid plaques in a mouse model of Alzheimer's disease.* Science, 2008. **321**(5896): p. 1686-9.
23. Le Meur, K., et al., *GABA release by hippocampal astrocytes.* Front Comput Neurosci, 2012. **6**: p. 59.
24. Banuelos, C., et al., *Prefrontal cortical GABAergic dysfunction contributes to age-related working memory impairment.* J Neurosci, 2014. **34**(10): p. 3457-66.
25. Mitew, S., et al., *Altered synapses and gliotransmission in Alzheimer's disease and AD model mice.* Neurobiol Aging, 2013. **34**(10): p. 2341-51.
26. Mei, Y.Y., D.C. Wu, and N. Zhou, *Astrocytic Regulation of Glutamate Transmission in Schizophrenia.* Front Psychiatry, 2018. **9**: p. 544.
27. Wang, K., et al., *TNF-alpha promotes extracellular vesicle release in mouse astrocytes through glutaminase.* J Neuroinflammation, 2017. **14**(1): p. 87.
28. Palop, J.J., et al., *Aberrant excitatory neuronal activity and compensatory remodeling of inhibitory hippocampal circuits in mouse models of Alzheimer's disease.* Neuron, 2007. **55**(5): p. 697-711.
29. Busche, M.A., et al., *Critical role of soluble amyloid-beta for early hippocampal hyperactivity in a mouse model of Alzheimer's disease.* Proc Natl Acad Sci U S A, 2012. **109**(22): p. 8740-5.
30. Grienberger, C., et al., *Staged decline of neuronal function in vivo in an animal model of Alzheimer's disease.* Nat Commun, 2012. **3**: p. 774.
31. Palop, J.J. and L. Mucke, *Network abnormalities and interneuron dysfunction in Alzheimer disease.* Nat Rev Neurosci, 2016. **17**(12): p. 777-792.
32. Lerdkrai, C., et al., *Intracellular Ca(2+) stores control in vivo neuronal hyperactivity in a mouse model of Alzheimer's disease.* Proc Natl Acad Sci U S A, 2018. **115**(6): p. E1279-E1288.
33. Asavapanumas, N., et al., *Role of intracellular Ca(2+) stores for an impairment of visual processing in a mouse model of Alzheimer's disease.* Neurobiol Dis, 2019. **121**: p. 315-326.
34. Yang, Y., et al., *Molecular comparison of GLT1+ and ALDH1L1+ astrocytes in vivo in astroglial reporter mice.* Glia, 2011. **59**(2): p. 200-7.
35. Petzold, A., *Glial fibrillary acidic protein is a body fluid biomarker for glial pathology in human disease.* Brain Res, 2015. **1600**: p. 17-31.
36. Middeldorp, J. and E.M. Hol, *GFAP in health and disease.* Prog Neurobiol, 2011. **93**(3): p. 421-43.

37. Cerutti, S.M. and G. Chadi, *S100 immunoreactivity is increased in reactive astrocytes of the visual pathways following a mechanical lesion of the rat occipital cortex.* Cell Biology International, 2000. **24**(1): p. 35-49.
38. Steiner, J., et al., *S100B is expressed in, and released from, OLN-93 oligodendrocytes: Influence of serum and glucose deprivation.* Neuroscience, 2008. **154**(2): p. 496-503.
39. Norenberg, M.D., *Distribution of glutamine synthetase in the rat central nervous system.* J Histochem Cytochem, 1979. **27**(3): p. 756-62.
40. Sturchler-Pierrat, C., et al., *Two amyloid precursor protein transgenic mouse models with Alzheimer disease-like pathology.* Proc Natl Acad Sci U S A, 1997. **94**(24): p. 13287-92.
41. Herzig, M.C., et al., *Abeta is targeted to the vasculature in a mouse model of hereditary cerebral hemorrhage with amyloidosis.* Nat Neurosci, 2004. **7**(9): p. 954-60.
42. Sturchler-Pierrat, C. and M. Staufenbiel, *Pathogenic mechanisms of Alzheimer's disease analyzed in the APP23 transgenic mouse model.* Ann N Y Acad Sci, 2000. **920**: p. 134-9.
43. Radde, R., et al., *Abeta42-driven cerebral amyloidosis in transgenic mice reveals early and robust pathology.* EMBO Rep, 2006. **7**(9): p. 940-6.
44. Bentahir, M., et al., *Presenilin clinical mutations can affect gamma-secretase activity by different mechanisms.* J Neurochem, 2006. **96**(3): p. 732-42.
45. Kuchibhotla, K.V., et al., *Synchronous hyperactivity and intercellular calcium waves in astrocytes in Alzheimer mice.* Science, 2009. **323**(5918): p. 1211-5.
46. Brawek, B., et al., *A bell-shaped dependence between amyloidosis and GABA accumulation in astrocytes in a mouse model of Alzheimer's disease.* Neurobiol Aging, 2018. **61**: p. 187-197.
47. Rodriguez, J.J., et al., *Complex and region-specific changes in astroglial markers in the aging brain.* Neurobiol Aging, 2014. **35**(1): p. 15-23.
48. Godbout, J.P., et al., *Exaggerated neuroinflammation and sickness behavior in aged mice after activation of the peripheral innate immune system.* Faseb Journal, 2005. **19**(7): p. 1329-+.
49. Sierra, A., et al., *Microglia derived from aging mice exhibit an altered inflammatory profile.* Glia, 2007. **55**(4): p. 412-424.
50. von Bernhardi, R., J.E. Tichauer, and J. Eugenin, *Aging-dependent changes of microglial cells and their relevance for neurodegenerative disorders.* J Neurochem, 2010. **112**(5): p. 1099-114.
51. Kimelberg, H.K., *Astrocyte Heterogeneity or Homogeneity?*, in *Astrocytes in (Patho)Physiology of the Nervous System*. 2009. p. 1-25.
52. Oberheim, N.A., S.A. Goldman, and M. Nedergaard, *Heterogeneity of astrocytic form and function.* Methods Mol Biol, 2012. **814**: p. 23-45.
53. Song, H., C.F. Stevens, and F.H. Gage, *Astroglia induce neurogenesis from adult neural stem cells.* Nature, 2002. **417**(6884): p. 39-44.

54. Grosche, A., et al., *Versatile and simple approach to determine astrocyte territories in mouse neocortex and hippocampus.* PLoS One, 2013. **8**(7): p. e69143.
55. Acaz-Fonseca, E., et al., *Regulation of astroglia by gonadal steroid hormones under physiological and pathological conditions.* Prog Neurobiol, 2016. **144**: p. 5-26.
56. Oakley, H., et al., *Intraneuronal beta-amyloid aggregates, neurodegeneration, and neuron loss in transgenic mice with five familial Alzheimer's disease mutations: potential factors in amyloid plaque formation.* J Neurosci, 2006. **26**(40): p. 10129-40.
57. Siwek, M.E., et al., *Altered theta oscillations and aberrant cortical excitatory activity in the 5XFAD model of Alzheimer's disease.* Neural Plast, 2015. **2015**: p. 781731.
58. Minkeviciene, R., et al., *Amyloid beta-induced neuronal hyperexcitability triggers progressive epilepsy.* J Neurosci, 2009. **29**(11): p. 3453-62.
59. Lerdkrai, C. and O. Garaschuk, *Role of presynaptic calcium stores for neural network dysfunction in Alzheimer's disease.* Neural Regen Res, 2018. **13**(6): p. 977-978.
60. Busche, M.A. and A. Konnerth, *Impairments of neural circuit function in Alzheimer's disease.* Philos Trans R Soc Lond B Biol Sci, 2016. **371**(1700).
61. Busche, M.A., et al., *Tau impairs neural circuits, dominating amyloid-beta effects, in Alzheimer models in vivo.* Nat Neurosci, 2019. **22**(1): p. 57-64.

8. Declaration of ownership

This thesis work has been performed at the Institute of Physiology, Department of Neurophysiology of the Eberhard-Karls-Universität Tübingen under guidance of Prof. Dr. Olga Garaschuk.

The majority of stainings and recordings and the analysis of all experiments have been performed by me (after introduction by laboratory staff E. Zirdum and A. Weible). Organ removal has been performed by B. Brawek or under her supervision. Immunhistochemical stainings have partially been performed by R. Chesters and E. Zirdum.

Statistical analysis was carried out by me after introduction by Dr. Brawek.

I declare that I have produced this work on my own (without external help), have only used the sources and aids indicated and have marked passages included from other works as such.

I have obtained the other Co-authors permission to cite the original publication.

Höchberg,

9. Publications

B. Brawek, R. Chesters, D. Klement, J. Müller, C. Lerdkrai, M. Hermes, and O. Garaschuk – “A bell-shaped dependence between amyloidosis and GABA accumulation in astrocytes in a mouse model of Alzheimer's disease.” - Neurobiol Aging – 2018 – Volume 6, Issue 61 – p. 187-197 [46]

10. Acknowledgements

I would like to thank Prof. Garaschuk for allowing me the opportunity to conduct my doctoral thesis project in her lab. I would also like to thank her for all the help and advice she has given me during my stay in her lab.

I too would like to thank Dr. Bianca Brawek for all her help with my project. For help with analysis and for her comments and corrections regarding my thesis manuscript and also encouragement.

I am also grateful for the technical support offered by Elizabeth Zirdum and Andrea Weible.

My gratitude also extends to all other members of the lab for all your help and advice.

Last but not least I would like to thank my family for constant support and encouragement.